

# Second measurements for seagrass and mangrove area cover in the four Marine and Coastal Priority Protected Areas (MCPAs) of Phase I of the MAR Fund Project

## Port Honduras Marine Reserve, Belize

Contract Services No. 08-2016 "CONSERVATION OF MARINE RESOURCES IN  
CENTRAL AMERICA" Project (Financial Agreement BMZ 2007 66 667)

Final Report – July 2017



©Matthias Stängel, RSS GmbH (Seagrass at Tobacco Caye, Belize, April 2016)

### **RSS – Remote Sensing Solutions GmbH**

Isarstr. 3  
82065 Baierbrunn/München  
Germany  
[www.rssgmbh.de](http://www.rssgmbh.de)  
[info@rssgmbh.de](mailto:info@rssgmbh.de)

Dr. Uwe Ballhorn, Dr. Claudius Mott,  
Elizabeth Atwood,  
Prof. Dr. Florian Siegert





## Table of Contents

<b>1. Introduction .....</b>	<b>2</b>
<b>2. Objectives.....</b>	<b>3</b>
<b>3. Project Area.....</b>	<b>4</b>
<b>4. Data and Methods.....</b>	<b>6</b>
4.1 Remote Sensing Data .....	6
4.2 Data Preprocessing.....	15
4.3 Object-based Classification Approach.....	17
4.4 Change Detection.....	22
<b>5. Results .....</b>	<b>23</b>
<b>6. Accuracy Assessment .....</b>	<b>32</b>
<b>7. Deliverables.....</b>	<b>36</b>
<b>Conclusions .....</b>	<b>37</b>
<b>References.....</b>	<b>38</b>
<b>Annex I.....</b>	<b>40</b>
<b>Annex II .....</b>	<b>54</b>

## 1. Introduction

The Mesoamerican Reef Fund (MAR Fund) was created to support the conservation and sustainable use of natural resources in the eco-region of the Mesoamerican Reef (MAR) shared between Belize, Guatemala, Honduras and Mexico. It is comprised of four founder funds, representing each of the MAR countries: Protected Areas Conservation Trust (PACT) in Belize, Fundación de los Recursos Naturales y Ambiente (FCG) in Guatemala, Fundación Biosfere (FB) in Honduras and Mexican Fund for the Conservation of Nature (FMCN) in Mexico.

The main focus of MAR Fund's grants programme is the development of an interconnected network of priority conservation areas. Simultaneously, MAR Fund seeks to address issues that directly affect the integrity and health of the network.

As part of the functional network programme for marine and coastal protected areas, implementation of the project "Conservation of Marine Resources in Central America – Phase I" is underway. This project supports best management practices, community participation in the conservation and sustainable use of coastal and marine resources in the initial network of protected areas within MAR. Funded by the German Government through Kreditanstalt für Wiederaufbau or KfW, the project is governed by both the Financial Contribution Contract signed on 8 December 2010 by MAR Fund and KfW, and the Separate Agreement signed on 29 March 2011.

The project will seek to consolidate selected protected areas in accordance with conservation priority criteria and to ensure the sustainable use of natural resources in adjacent coastal and marine areas in the medium term, in an effort to preserve the ecological functions of the MAR. The criteria for achieving these objectives, project outcomes and the assumptions underlying the objectives and results of the project are defined within the project's Logical Framework.

Total contributions for the project come to €6.1 million. KfW contributes €5 million. Protected areas and beneficiaries will contribute €1,320,252, while the remainder of the budget will come from existing budgets for the protected areas and from funds provided by the MAR Fund and its members.

The project was estimated to last five years from January 2012. However, the project was benefited with an eight-month time extension.

TYPSA was selected and contracted to deliver technical assistance to the project.

The following objectives are defined:

(a) Main objective

To contribute to conservation of the ecological functions of the Mesoamerican Reef System

(b) Project objective

To consolidate selected Marine and Coastal Protected Areas (MCPA) in the project's region and to ensure the conservation and sustainable use of marine and coastal resources in the medium term

The project area is bounded by the Mesoamerican Reef System (MAR), shared between Mexico, Belize, Guatemala and Honduras. These coastal and marine ecosystems are remarkable in their biological diversity and provide a variety of ecosystem services to the adjoining nations. Ecosystem services include benefits such as shelter from tropical storms, reef fisheries, sustainment of biodiversity, a prosperous tourism industry or the provision of building materials. Besides coral reefs, mangrove and seagrass habitats are an integral component of the coastal ecosystem.

Consequent monitoring of ecosystems in the MAR is inevitable for preventing the continuing rapid loss of those habitats. Many studies and initiatives have demonstrated the high potential of remote sensing techniques for assessing coastal habitats like seagrass canopies (Dekker et al. 2006, Mumby et al. 1997) or mangroves (Green et al. 2004, Giri et al. 2011, Kuenzer et al. 2011), health status and potential stress parameters in coastal ecosystems. Mapping those ecosystems via remote sensing using aerial and satellite sensors has been shown to be more cost-effective than fieldwork (Mumby et al. 1999, Mumby et al 1997).

The following Marine and Coastal Priority Protected Areas (MCPA) are the main investment areas for Phase I of the project:

1. Yum Balam Protection Area for Flora and Fauna, Mexico (154,050 ha)
2. Port Honduras Marine Reserve, Belize (40,499 ha)
3. Punta de Manabique Wildlife Refuge, Guatemala (129,848 ha)
4. Sandy Bay-West End Special Marine Protection Zone, Honduras (2,153 ha)

The outcome of this consultation was to provide current status (2016) of the coverage in all four areas through a second measurement phase, and a comparison between the baseline (2013) and this new measurement information.

The present report describes the procurement, preprocessing and classification of high resolution RapidEye, Sentinel-2A and Landsat 8 satellite imagery for the project area MCPA **Port Honduras Marine Reserve**, Belize. RSS - Remote Sensing Solutions GmbH - generated mangrove and seagrass cover maps that represent the 2016 cover status in the project area at a high spatial level of detail. These mangrove and seagrass cover maps provide information on different density classes and were compared to the mangrove and seagrass baseline maps from 2013. Through this comparison it can be determined whether the two main objective indicators of the MAR Fund have been accomplished at the end of the project:

- Areas of mangroves in project MCPA equal to or greater than the baseline
- Areas of marine seagrass beds in project MCPA equal to or greater than the baseline

These two main objective indicators are impact indicators and are used to measure the overall positive impact in each area through the implementation of the project.

## 2. Objectives

The objectives of the study are:

- Derivation of a reliable up-to-date (2016) coverage using actual RapidEye, Sentinel-2A and Landsat 8 satellite imagery
- Application of consistent state of the art classification methodologies
- Plausibility checks and accuracy assessment implemented by experts
- The following information is provided:
  - Mangrove area in the Port Honduras Marine Reserve (Belize) from the year 2016 – assessed at a reliable quality and comparable methodology

- Seagrass area in the Port Honduras Marine Reserve (Belize) from the year 2016 – assessed at a reliable quality and comparable methodology
- Comparative analysis of these up-to-date mangrove and seagrass maps with the ones derived for the year 2013

This assessment will serve to determine whether the objectives of the MAR Fund have been accomplished at the end of the project.

### **3. Project Area**

In 2000 the Port Honduras Marine Reserve was established by the Government of Belize and is currently co-managed by the Toledo Institute for Development and Environment (TIDE) and the Fisheries Department. With 40,499 ha it is Belize's second largest Marine Reserve and forms part of the ecologically important Maya Mountain Corridor complex (Figure 1; Cherrington 2013).

The Belize Barrier Reef System (within the Mesoamerican Reef Ecoregion) is the largest barrier reef system in the Americas and is comprised of an assemblage of interconnected mangrove, seagrass, and coral reef ecosystems (Cherrington 2013).

Of the coastal marine ecosystems, mangroves and seagrass meadows are considered to be among the most productive (McField and Kramer 2007; Wabnitz et al. 2007). As in the whole Caribbean mangroves and seagrass meadows are threatened by coastal infrastructure development and a range of other development pressures (McField and Kramer 2007). Therefore baseline studies of mangrove and seagrass distribution are important as damages in these ecosystems have direct and indirect negative effects on different environmental services such as: breeding areas for fish populations, reproduction, refuge, nesting, growth of different species, source of organic matter, beach stability, and capture-, stabilization-, and formation of sediments. Extended knowledge of existence, quantity, quality, and distribution of mangroves and seagrass is indispensable to suggest adequate laws, develop strategic plans and cost / benefit assessments.



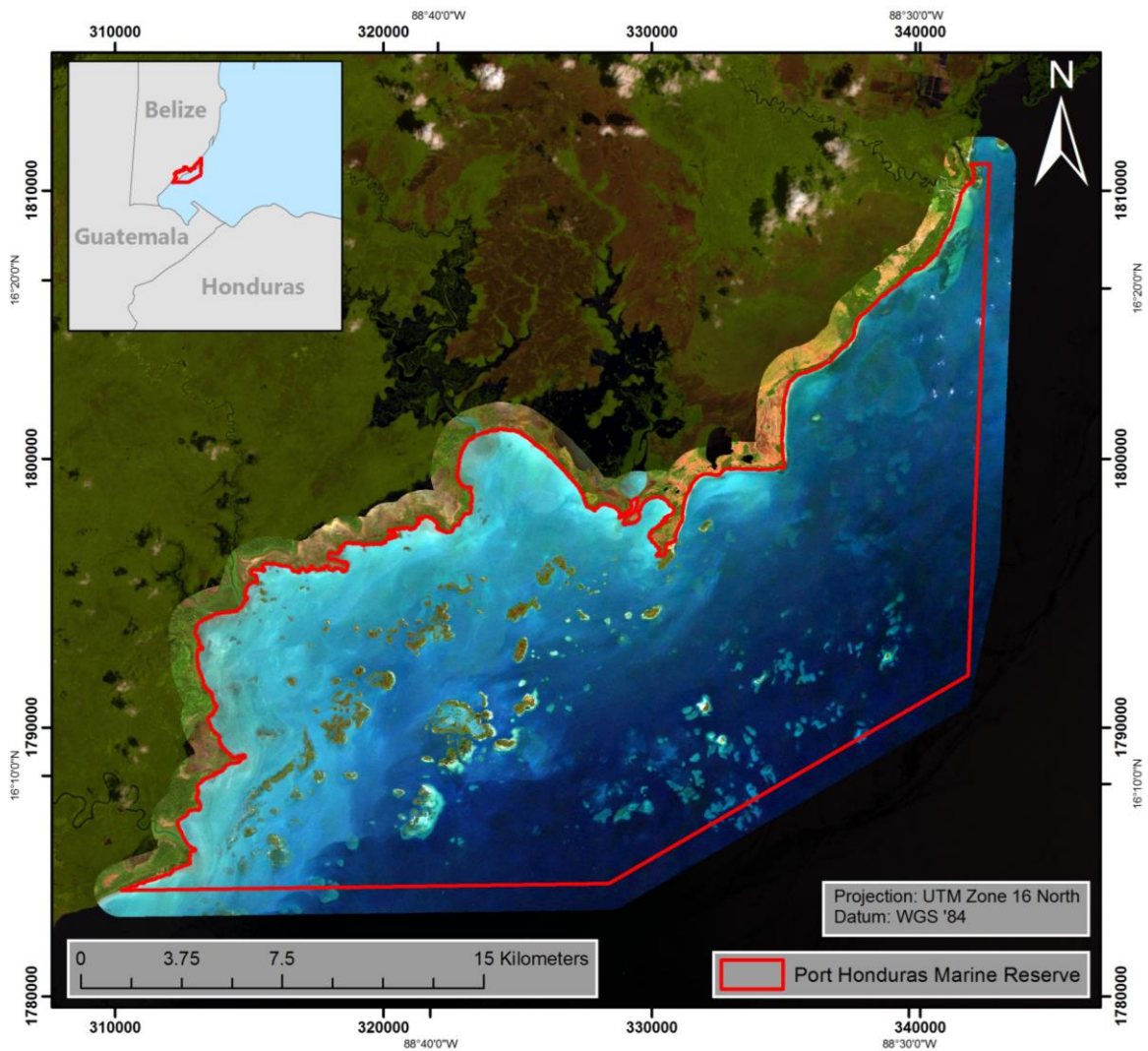


Figure 1: Overview of the Port Honduras Marine Reserve (Belize). True-color RapidEye imagery (02/02/2016) superimposed on Sentinel-2A data (11/03/2016; bands: short wavelength infrared (band 11), near infrared (band 8), and red (band 4)). The border of Port Honduras Marine Reserve is displayed in red.

## 4. Data and Methods

### 4.1 Remote Sensing Data

Three sources of remote sensing data were used:

#### RapidEye constellation

The generation of high resolution land cover/vegetation type maps that also take different vegetation density classes into account require specific data characteristics and image analysis techniques. RSS therefore used data of the advanced satellite system constellation RapidEye, which provides high-resolution imagery within very short revisit times. The RapidEye satellite system, launched in August 2008, is a constellation of five identical satellites and thus has the unique ability to acquire high-resolution image data with 5 spectral bands on an almost daily basis (Table 1). Its spatial resolution is 6.5 m, which is resampled to 5 m during preprocessing by the data provider. Being able to collect more than 4 million km<sup>2</sup> of data per day as a constellation, each satellite can acquire imagery in 77 km-wide swaths extending at least 1,500 km in length. RapidEye has imaged more than 2 billion km<sup>2</sup> of the Earth's surface since February 2009.

Table 1: Characteristics of the RapidEye satellite constellation (Source: Planet Labs).

<b>Mission Characteristics</b>	<b>Information</b>	
Number of satellites	5	
Spacecraft lifetime	Over 7 years	
Orbit altitude	630 km in sun-synchronous orbit	
Equator crossing time	11:00 am local time (approximately)	
Sensor type	Multi-spectral push broom imager	
Spectral bands	Capable of capturing all of the following spectral bands:	
	<u>Band Name</u>	<u>Spectral Range (nm)</u>
	Blue	440-510
	Green	520-590
	Red	630-685
	Red edge	690-730
NIR	760-850	
Ground sampling distance (nadir)	6.5 m	
Pixel size (orthorectified)	5 m	
Swath width	77 km	
On board data storage	Up to 1,500 km of image data per orbit	
Revisit time	Daily (off-nadir) / 5.5 days (at nadir)	
Image capture capacity	5 million km <sup>2</sup> /day	
Camera dynamic range	12 bit	

The high temporal repetition rate of RapidEye is of vital importance in regions with frequent cloud cover and short dry seasons, since it increases the probability of area coverage with acceptable cloud cover and thus makes detailed monitoring possible. RapidEye data is particularly suitable to precisely assess forest cover and forest status since their spectral, spatial and temporal characteristics allow for a repetitive monitoring of tropical forests at high spatial detail (Figure 2).



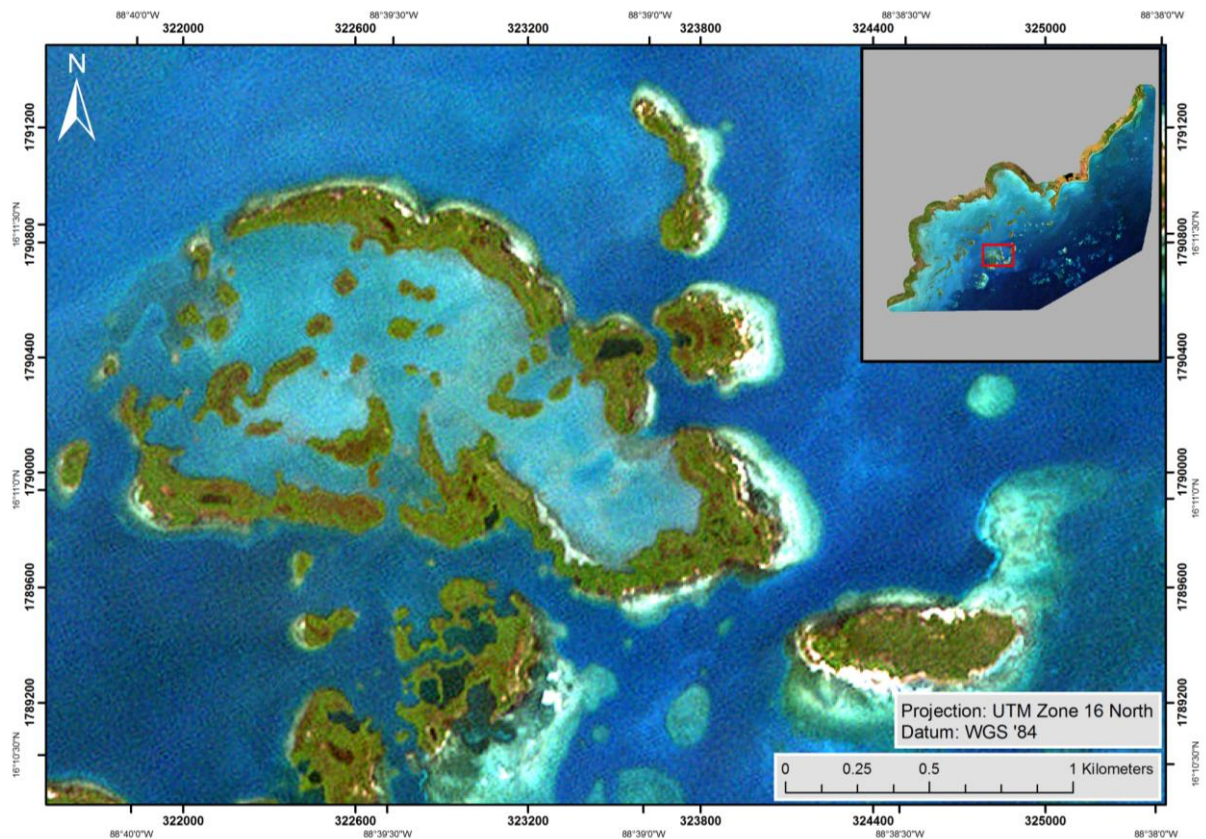


Figure 2: Subset of a RapidEye image (true-color) showing the spatial detail in land cover. The red rectangle in the upper right image shows the location of the subset within the Port Honduras Marine Reserve.

In the present study, Level 3A RapidEye imagery was used. This orthorectified product is provided as 25 km by 25 km tiles. Radiometric, sensor and geometric correction is applied to the data (Table 2). More detailed information on the data product is provided in the Satellite Imagery Product Specification from Planet Labs available at:

[https://www.planet.com/assets/themes/planet/pdf/1601.RapidEye.Image.Product.Specs\\_Jan16\\_V6.1\\_ENG.pdf](https://www.planet.com/assets/themes/planet/pdf/1601.RapidEye.Image.Product.Specs_Jan16_V6.1_ENG.pdf) (February 2017)

Table 2: Level 3A RapidEye product specifications.

Product Attribute	Description
Product Components and Format	RapidEye Ortho image product consists of the following components: Image File – GeoTIFF file that contains image data and geolocation information Metadata File – XML format metadata file Browse Image File – GeoTIFF format Unusable Data Mask (UDM) file – GeoTIFF format
Product Orientation	Map North up
Product Framing	Image Tile (image tiles are based on a worldwide, 24km by 24km grid system). To each 24km by 24km grid square, a 500m overlap is added to produce a 25km by 25km image tile. Image tiles are black-filled 1km beyond the order polygon used during order placement. Tiles only partially covered an image take will be also black-filled in areas containing no valid image data.
Pixel Spacing	5m
Bit Depth	16-bit unsigned integers.
Product Size	Tile size is 25km (5000lines) by 25km (500 columns). 250 Mbytes per tile for 5 bands at 5m pixel spacing.
Geometric Corrections	Sensor-related effects are corrected using sensor telemetry and sensor model, bands are co-registered, and spacecraft-related effects are corrected using attitude telemetry and best available ephemeris data. Orthorectified using GCPs and fine DEMs (30m to 90m posting).
Horizontal Datum	WGS84
Map Projection	Universal Transverse Mercator (UTM)
Resampling Kernel	Cubic Convolution (default), MTF, or Nearest Neighbor

Level 3A RapidEye data from 02/02/2016 was used for the mangrove and seagrass classification of the Port Honduras Marine Reserve. Figure 3 displays this almost cloud free imagery.

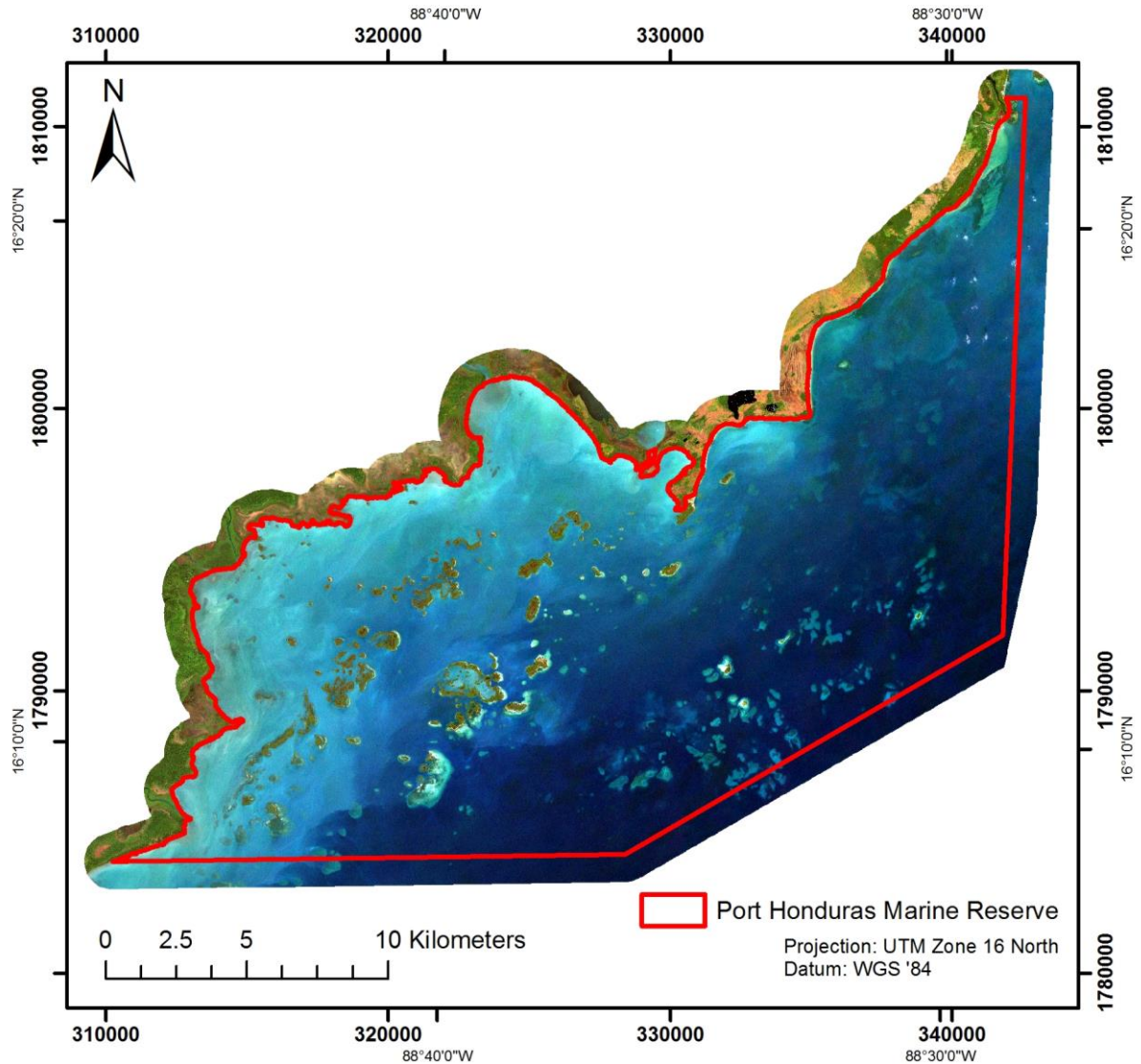


Figure 3: Figure 3: True-color RapidEye imagery (02/02/2016) used for the mangrove and seagrass mapping.

### Sentinel-2A

The Sentinel-2 mission is based on a constellation of two satellites, both orbiting Earth at an altitude of 786 km but 180° apart. This configuration optimises coverage and global revisit times. Sentinel-2A was launched on 23 June 2015 and Sentinel-2B was launched in March 2017. The instrument on-board Sentinel-2A is a multispectral imager (MSI) covering 13 spectral bands (443 nm – 2,190 nm) with a swath width of 290 km and a spatial resolution of 10 m (4 visible and near infrared bands), 20 m (6 red edge/short wavelength infrared bands) and 60 m (3 atmospheric bands). Table 3 gives an overview of the Sentinel-2A data specifications. More detailed information on Sentinel-2A data is provided at:

[http://www.esa.int/Our\\_Activities/Observing\\_the\\_Earth/Copernicus/Sentinel-2](http://www.esa.int/Our_Activities/Observing_the_Earth/Copernicus/Sentinel-2).

Sentinel-2A is free of charge and available via the ESA Copernicus Open Access Hub (<https://scihub.copernicus.eu/dhus/#/home>) (February 2017).

Table 3: Sentinel-2A product specifications.

Sentinel-2A bands	Central wavelength ( $\mu\text{m}$ )	Spatial resolution (m)
Band 1 – Coastal aerosol	0.443	60
Band 2 – Blue	0.490	10
Band 3 – Green	0.560	10
Band 4 – Red	0.665	10
Band 5 – Vegetation red edge	0.705	20
Band 6 – Vegetation red edge	0.740	20
Band 7 – Vegetation red edge	0.783	20
Band 8 – NIR	0.842	10
Band 8A – Vegetation red edge	0.865	20
Band 9 – Water vapour	0.945	60
Band 10 – SWIR – cirrus	1.375	60
Band 11 – SWIR	1.610	20
Band 12 – SWIR	2.190	20

Especially due to the red-edge and short wavelength infrared bands Sentinel-2A data has proven to be very appropriate for investigating forest ecosystems (<https://earth.esa.int/web/sentinel/missions/sentinel-2/news/-/article/sentinels-accelerate-monitoring-of-forest-change>, March 2017) like mangroves (Figure 4).

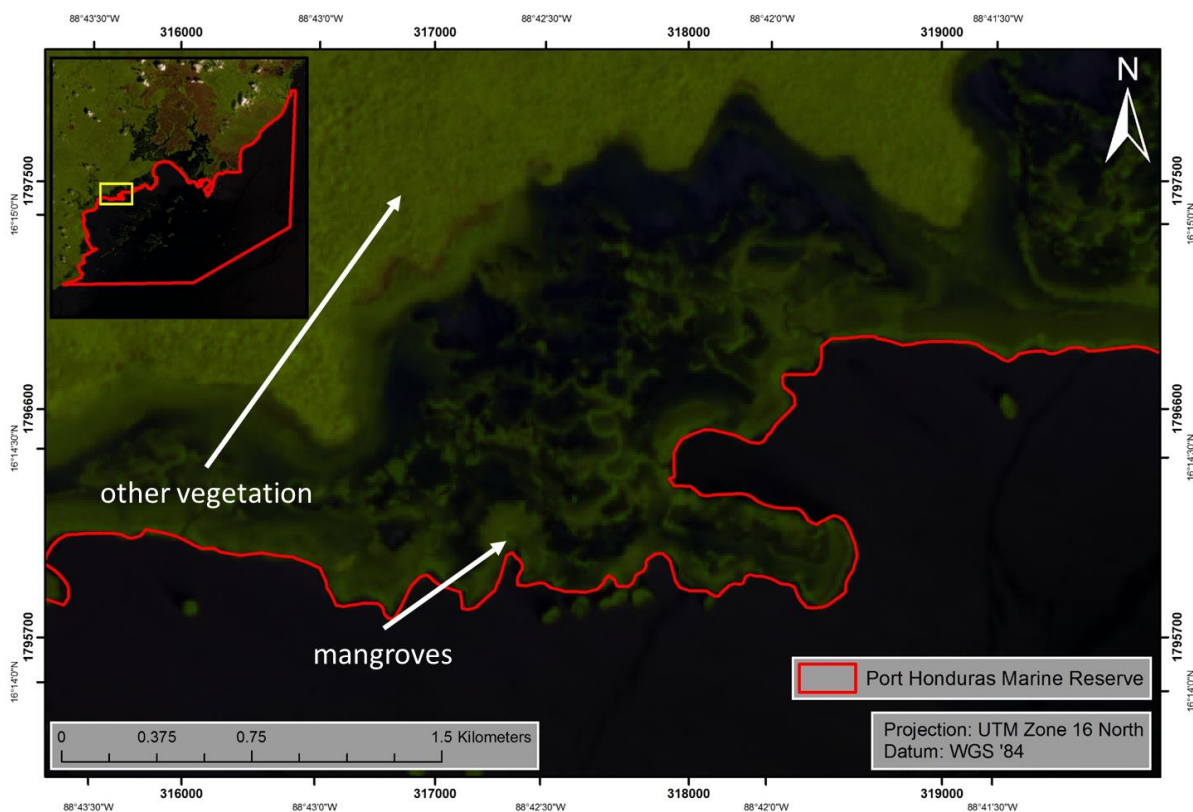


Figure 4: Subset of a Sentinel-2A imagery (11/03/2016; bands: short wavelength infrared (band 11), near infrared (band 8), and red (band 4) showing that mangroves can be differentiated from other vegetation types. The yellow rectangle in the upper left image shows the location of the subset within the Port Honduras Marine Reserve.



The Sentinel-2A archive was checked and the most appropriate imagery (11/03/2016) downloaded. Figure 5 shows the acquired Sentinel-2A data for the Port Honduras Marine Reserve.

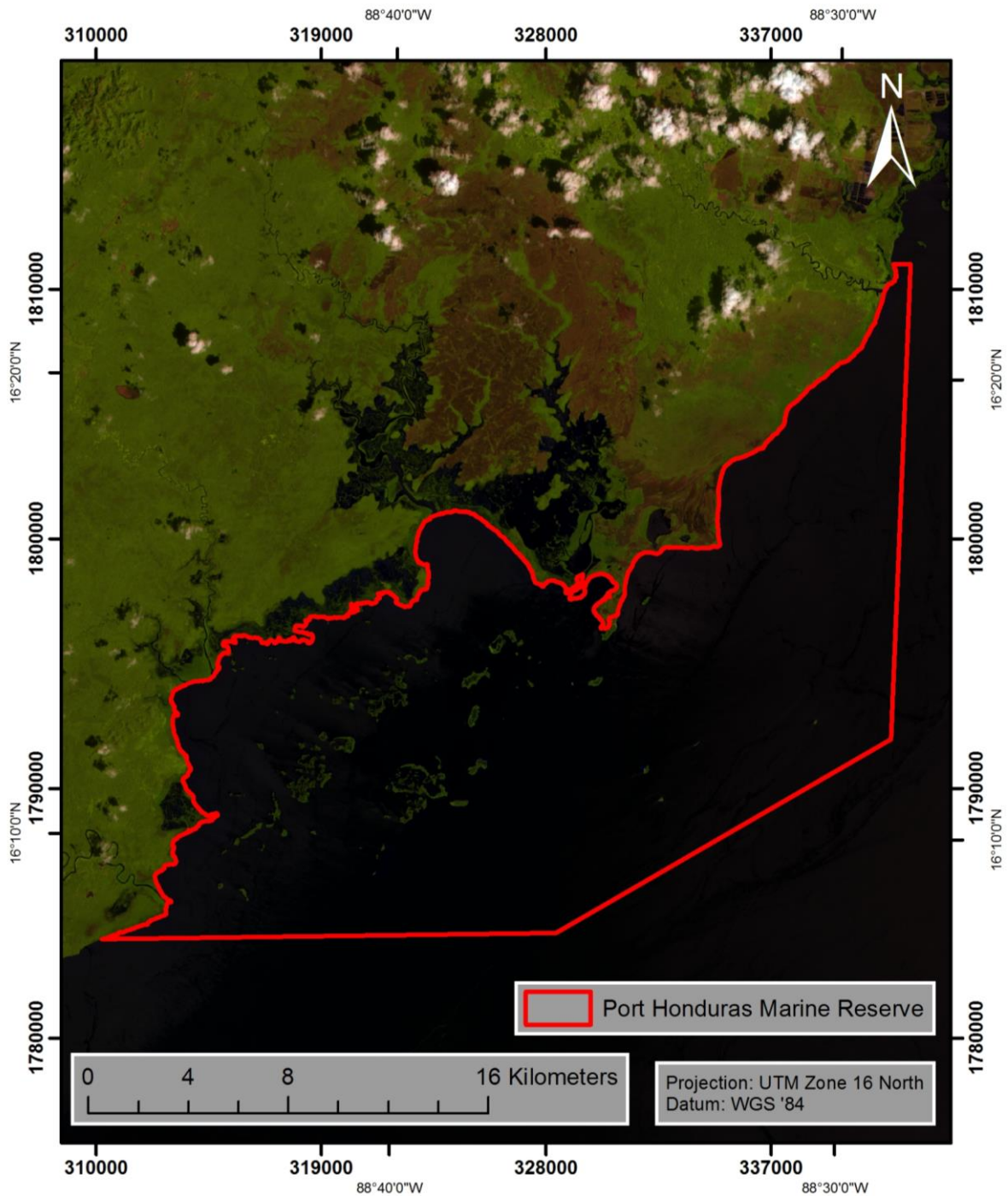


Figure 5: Sentinel-2A imagery (11/03/2016; bands: short wavelength infrared (band 11), near infrared (band 8), and red (band 4) used for the mangrove and seagrass mapping.

## Landsat 8

Landsat 8 covers the Earth's surface along the satellite's ground track in a 185-kilometer-swath as the satellite moves in a descending orbit over the sunlit side of the Earth (USGS 2017). Landsat 8 orbits the earth at 705 km altitude. They cross every point on the Earth once every 16 days. The OLI on-board Landsat 8 collects data in nine shortwave bands – eight spectral bands at 30 m spatial resolution and one panchromatic band at 15 m. Refined heritage bands and the addition of a new coastal/aerosol band create data products with improved radiometric performance. OLI data products have a 16-bit range. Table 4 gives an overview of the Landsat 8 data specifications. More detailed information on Landsat 8 data is provided at: <https://landsat.usgs.gov/landsat8.php>. Landsat 8 data is free of charge and available from the U.S. Geological Survey (USGS) agency via their ftp server: <http://earthexplorer.usgs.gov/> (hyperlink assessed March 2017).

Table 4: Landsat 8 product specifications.

<b>Product Attribute</b>	<b>Description</b>
Processing	Level 1 T- Terrain Corrected
Pixel Size	OLI multispectral bands 1-7, 9: 30m OLI panchromatic band 8: 15m TIRS bands 10-11: collected at 100m but resampled to 30m to match OLI multispectral bands
Data Characteristics	<ul style="list-style-type: none"><li>• GeoTIFF data format</li><li>• Cubic Convolution (CC) resampling</li><li>• North Up (MAP) orientation</li><li>• Universal Transverse Mercator (UTM) map projection (Polar Stereographic projection for scenes with a center latitude greater than or equal to -63.0 degrees)</li><li>• World Geodetic System (WGS) 84 datum</li><li>• 12m circular error, 90% confidence global accuracy for OLI</li><li>• 41m circular error, 90% confidence global accuracy for TIRS</li><li>• 16-bit pixel values</li></ul>

Landsat data has proven to be very appropriate for detecting forest ecosystems like mangroves (Chen et al. 2013, Giri et al. 2011, Kuenzer et al. 2011) (Figure 6).



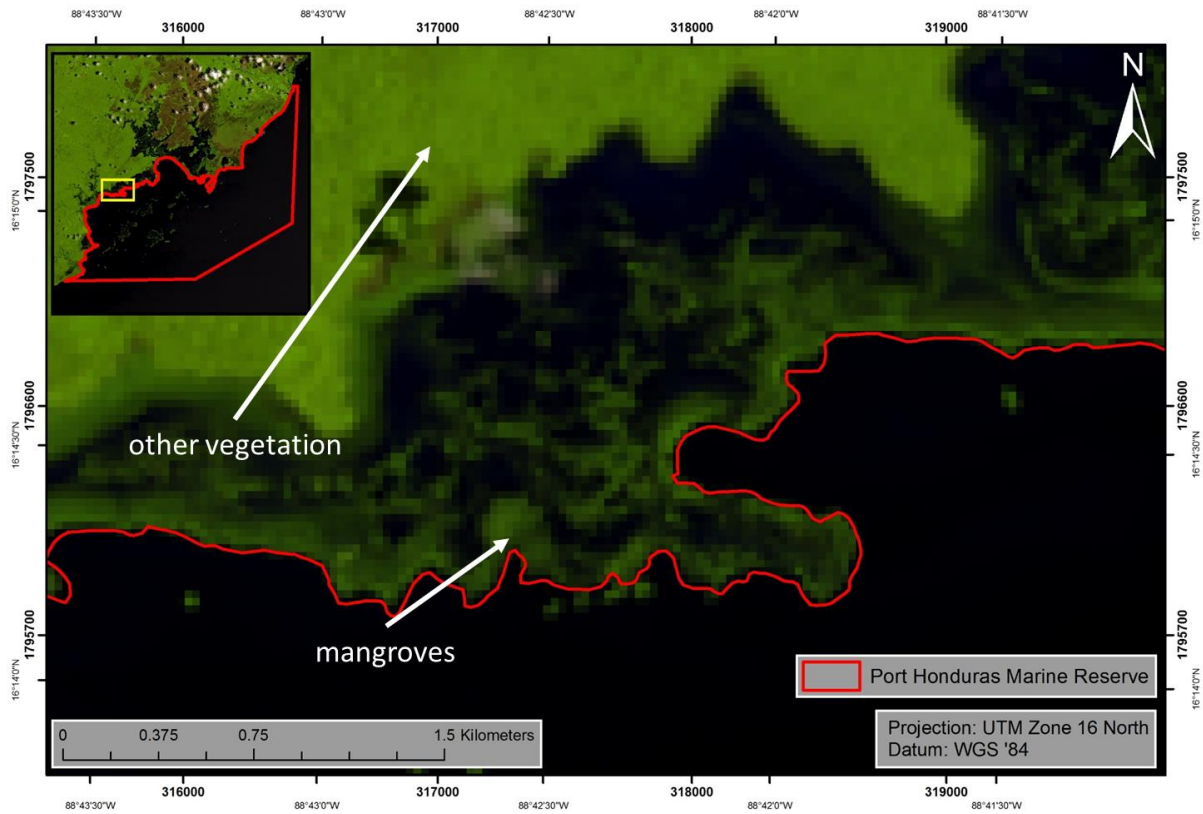


Figure 6: Subset of a Landsat 8 imagery (bands: short wavelength infrared (band 7), near infrared (band 5), and red (band 4) showing that mangroves can be differentiated from other vegetation types. The yellow rectangle in the upper right image shows the location of the subset within the Port Honduras Marine Reserve.

The Landsat 8 archive was checked and the most appropriate imagery (31/08/2016) downloaded. Figure 7 shows the acquired Landsat 8 data for the Port Honduras Marine Reserve.

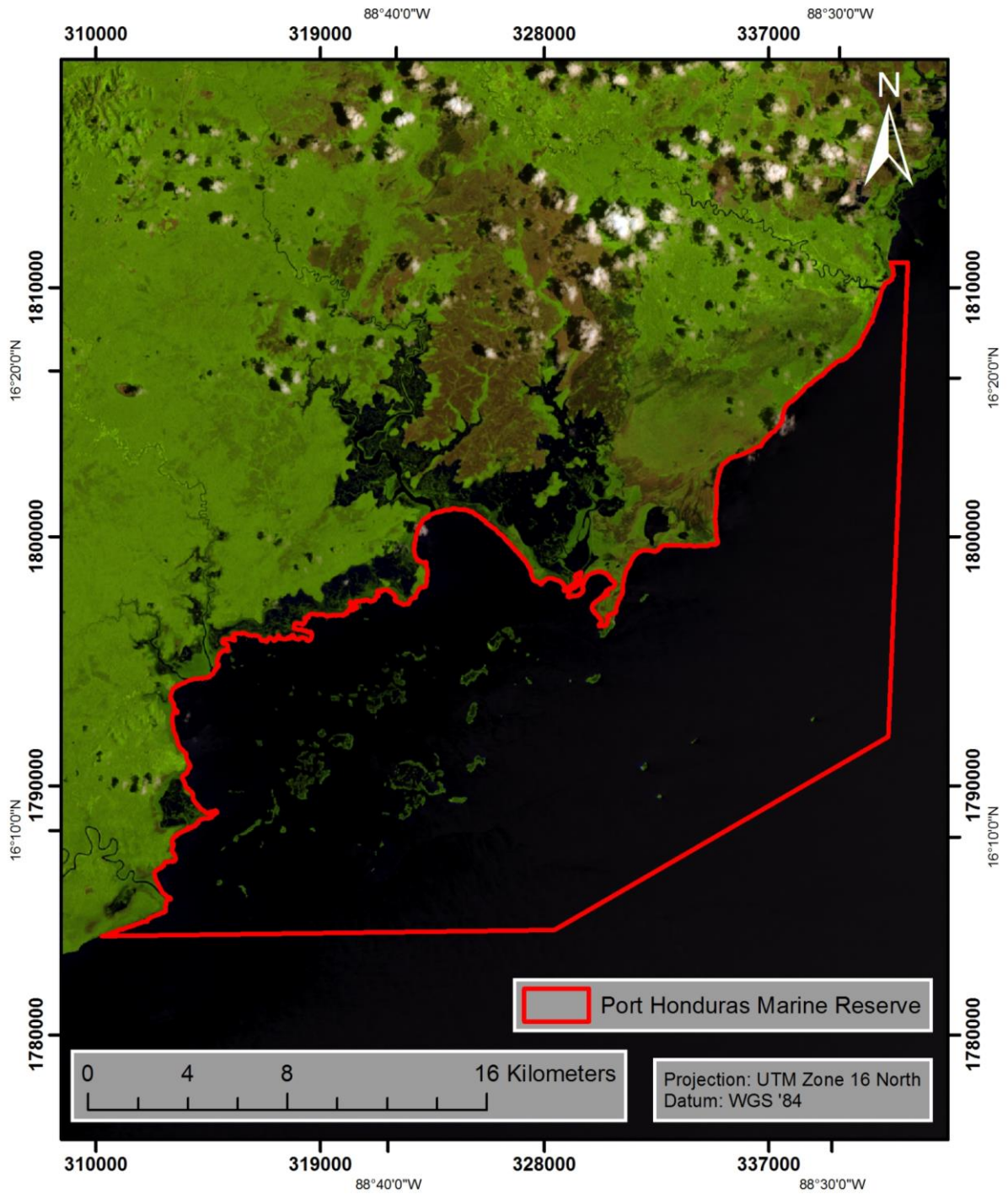


Figure 7: Landsat 8 scene (31/08/2016; bands: short wavelength infrared (band 7), near infrared (band 5), and red (band 4) used for the mangrove and seagrass mapping.

Table 5 gives an overview of the remote sensing data used for the mangrove and seagrass classification of the year 2016. Images with different acquisition dates within the year 2016 were used to get a preferably cloud free coverage of the study area. The subsequent classification rulesets were adapted according to the different vegetation periods.

Table 5: Overview of remote sensing data used for the mangrove and seagrass classification of the year 2016.

<b>Rapid Eye</b>		
<b>Amount tiles</b>	<b>Acquisition date</b>	<b>Cloud cover within study area (%)</b>
4 (level 3A)	02/02/2016	<1
<b>Sentinel-2A</b>		
<b>Amount images</b>	<b>Acquisition date</b>	<b>Cloud cover within study area (%)</b>
2	11/03/2016	0
<b>Landsat 8</b>		
<b>Amount images</b>	<b>Acquisition date</b>	<b>Cloud cover within study area (%)</b>
1	31/08/2016	<1

## 4.2 Data Preprocessing

An essential preprocessing step was the removal of atmospheric effects that influence the signal, induced by water vapour and aerosols in the atmosphere as well as varying sun illumination angles in different seasons. This preprocessing step results in the calibration of the data and allows an estimation of the surface reflectance without atmospheric distortion effects. The calibration method facilitates an improved scene-to-scene radiometric measurements comparability, which is a necessary precondition for the subsequent semi-automatic object-based rule-set classification method. The atmospheric correction was applied to each image using ATCOR-2 (Richter and Schläpfer 2011; [http://www.rese.ch/products/atcor/atcor3/atcor2\\_method.html](http://www.rese.ch/products/atcor/atcor3/atcor2_method.html)). The following parameters were used in ATCOR-2:

- Atm. Correction: pre-defined sensors, flat terrain
- Acquisition data of the satellite data
- Selection of sensor (RapidEye, Sentinel-2A or Landsat 8) and corresponding calibration file
- Atmospheric file: tropical maritime
- Satellite and sun geometry from the metadata of the satellite data
- Ground elevation: 0 km

Landsat 8 product specifications state that the OLI has a has a geolocation uncertainty of less than 12 m circular error (Table 4). Visual analysis showed that the Sentinel-2 and Landsat 8 data had an excellent geometrical fit with the RapidEye data so no geometrical co-registration was necessary. In Figure 8 the geometrical fit of the Sentinel-2A data (upper figure right) and Landsat 8 data (lower figure right) in comparison to RapidEye data is displayed (upper figure left and lower figure left). Exemplarily a river is shown. The river is spatially located at the same location within all shown datasets. Additionally, the two figures show, that the pixels exactly fit to each other.

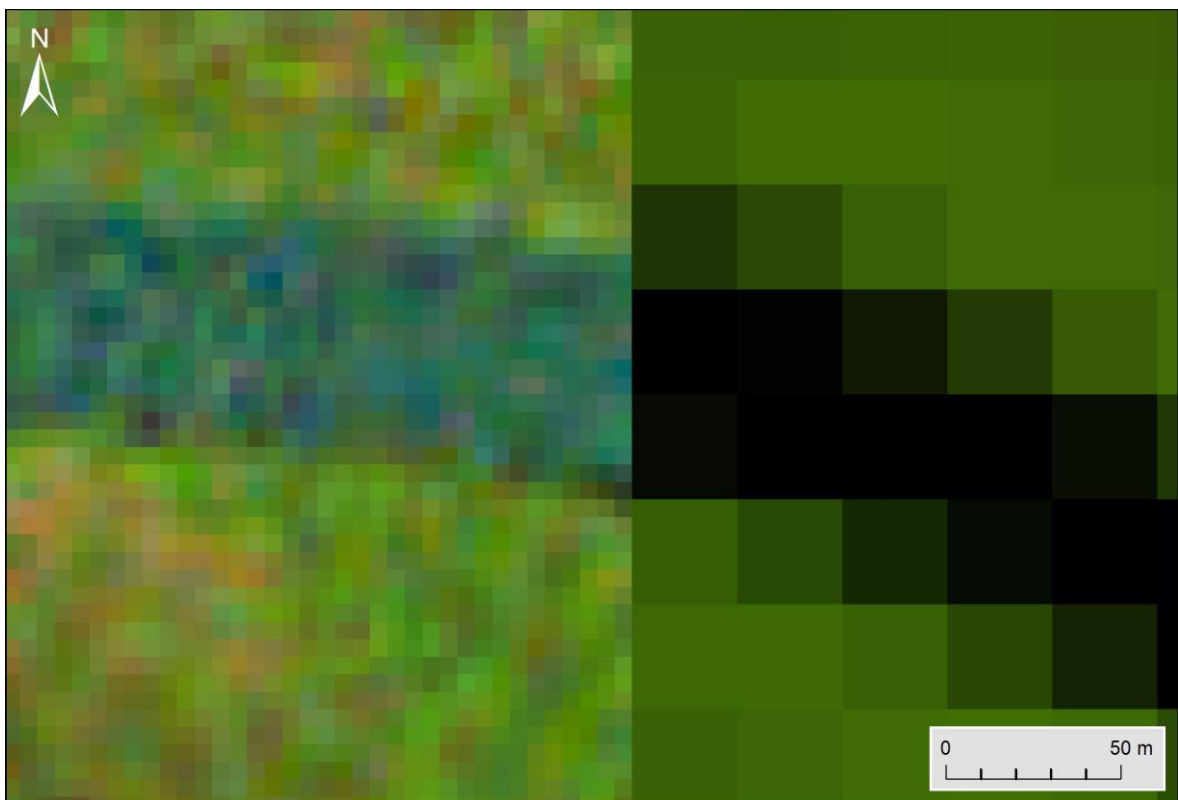
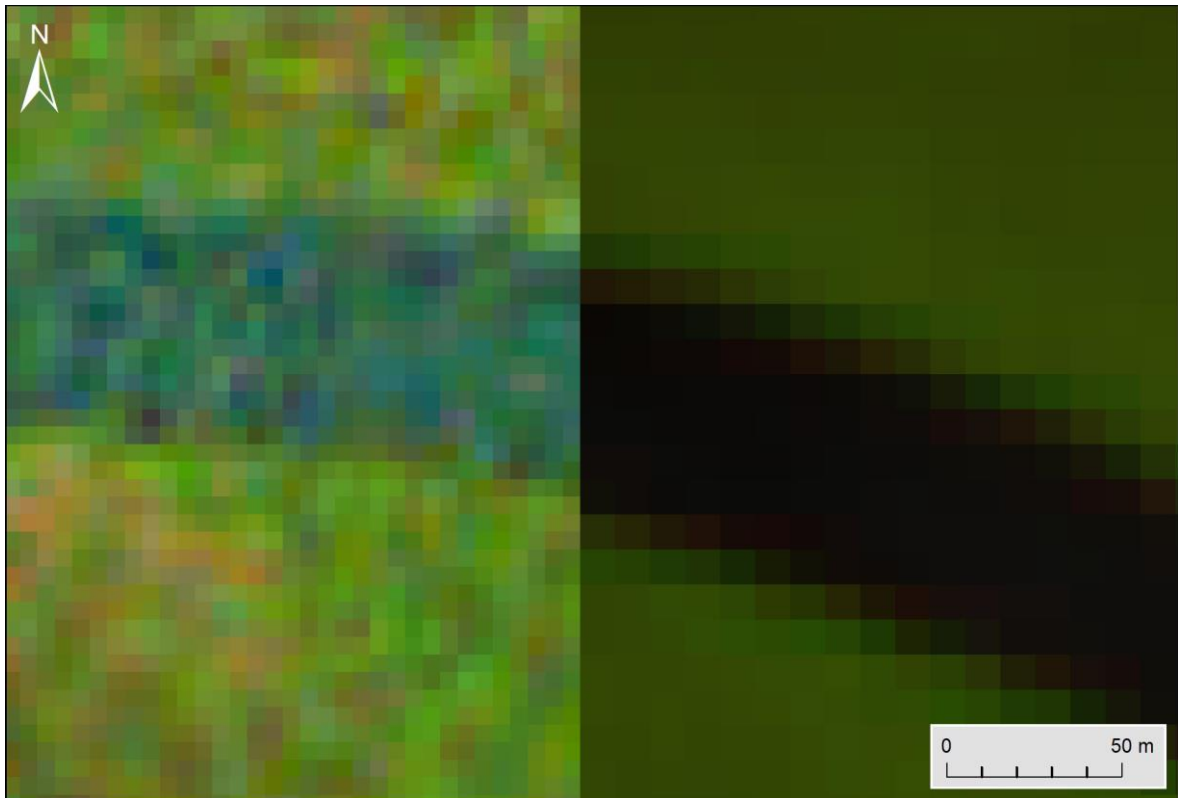


Figure 8: Geometrical fit of the Sentinel-2A data (upper figure right) and Landsat 8 data (lower figure right) in comparison to RapidEye data (upper figure left and lower figure left). Exemplarily a river is shown. The river is spatially located at the same location within all shown datasets. Additionally, the two figures show, that the pixels exactly fit to each other. Due to this no geometrical co-registration was necessary.

### 4.3 Object-based Classification Approach

The basic classification method was an object-based image analysis approach using eCognition software (Trimble Geospatial, Munich, Germany). This methodology classifies spatially adjacent and spectrally similar groups of pixels, so called image objects, rather than individual pixels of the image. Traditional pixel-based classification uses multi-spectral classification techniques that assign a pixel to a class by considering the spectral similarities with the class or with other classes. The resulting thematic classifications are often incomplete and non-homogeneous. The received signal frequency does not clearly indicate the membership to a land cover class, e.g. due to atmospheric scattering, mixed pixels, or the heterogeneity of natural land cover. Improved spatial resolution of remote sensing systems has resulted in increased complexity of the data. The representation of real world objects in the feature space is characterized by high variance of pixel values, hence statistical classification routines based on the spectral dimensions are limited and a greater emphasis must be placed on exploiting spatial and contextual attributes (Guindon 1997, Guindon 2000, Matsuyama 1987). To enhance classification, the use of spatial information inherent in such data was proposed and studied by many researchers (Atkinson and Lewis 2000). A lot of approaches make use of the spatial dependence of adjacent pixels. Approved routines are the inclusion of texture information, the analysis of the (semi-)variogram, or region growing algorithms that evaluate the spectral resemblance of proximate pixels (Hay et al. 1996, Kartikeyan et al. 1998, Woodcock et al. 1988). In this context, the use of object-oriented classification methods on remote sensing data has gained immense popularity, and the underlying idea has been subject to numerous investigations since the 1970's (Haralick and Joo 1986, Kartikeyan et al. 1995, Kettig and Landgrebe 1976)

The first step of the object-oriented approach is a segmentation of the imagery to generate image objects, where neighbouring pixel clusters are combined into an image object. Here the spectral reflectance, as well as texture information and shape indicators are analysed for generating the objects. The attributes of the image objects (such as spectral reflectance, texture or the Normalized Difference Vegetation Index NDVI) are stored in a so called object database (Benz 2004, Mott 2005). Classification itself corresponds in fact to a complex database query by formulating rule sets on how the object attributes should be evaluated. Additionally, expert knowledge can be implemented in the classification process.

This approach consists of three basic procedures (Figure 9):

- **Design of a class hierarchy:** Definition of classes and inheritance rules between parent and child classes
- **Image segmentation:** The input image raster dataset is segmented into homogeneous image objects according to their spectral and textural characteristics
- **Classification:** The image objects are assigned to the predefined classes according to decision rules which can be based on spectral, spatial, geometric, thematic or topologic criteria





RapidEye satellite image

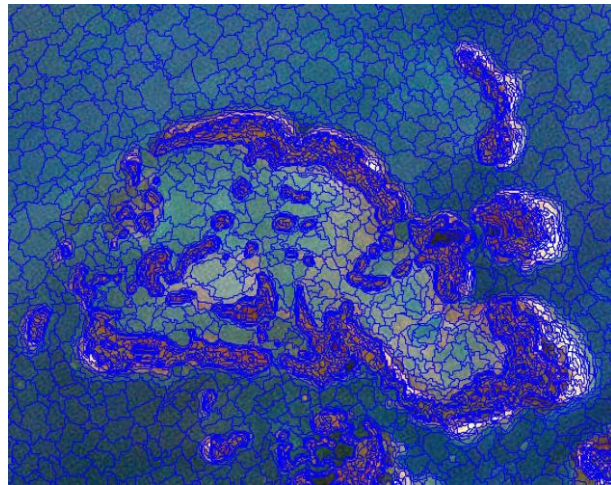
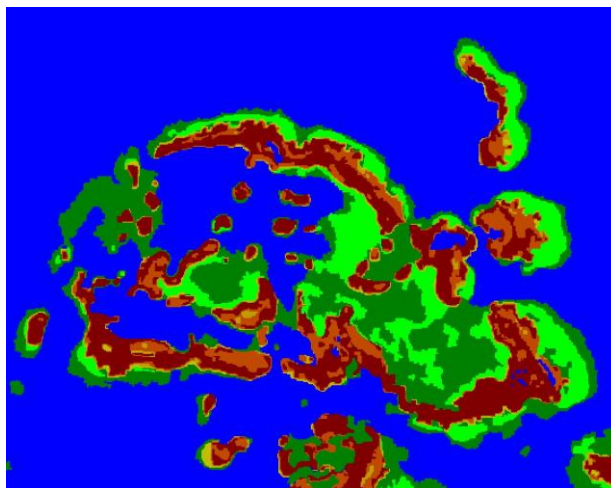


Image segmentation



- Mangroves 0-25
- Mangroves 25-50
- Mangroves 50-75
- Mangroves 75-100
- Seagrass 0-50
- Seagrass 50-100
- Water

Classification based on image object attributes

Figure 9: Example of the basic procedures of an object-based image analysis. The input image dataset (top) is first segmented into homogeneous image objects (middle) which are then assigned to predefined classes according to decision rules (down).



The first step in the classification process is the definition of the class hierarchy on the basis of the classification scheme. In total, 6 *ecological* classes were defined:

4 mangrove density classes:

1. 0-25%
2. 25-50%
3. 50-75%
4. 75-100%

2 seagrass density classes:

1. 0-50% seagrass coverage
2. 50-100% seagrass coverage

Originally a classification scheme stratifying 25% levels of coverage, meaning 0-25%, 25-50%, 50-75% and 75-100% seagrass coverage was proposed. The conducted analyses showed that such a fine distinction is not implementable with serious scientific standards. Due to turbidity of the ocean, esp. in shallow waters, very low seagrass coverages may not be reliably detected. Turbidity, caused by high concentrations of suspended matter in shallow waters, makes a reliable detection of isolated seagrass patches difficult. Total suspended matter can include a wide variety of material, such as silt, decaying plant and animal matter, industrial waste as well as sewage (Figure 10). Therefore, the classification scheme concerning seagrass was adjusted to two classes: Seagrass coverage, 0-50% and 50-100% seagrass coverage. The same classification scheme was used in the mapping 2013.

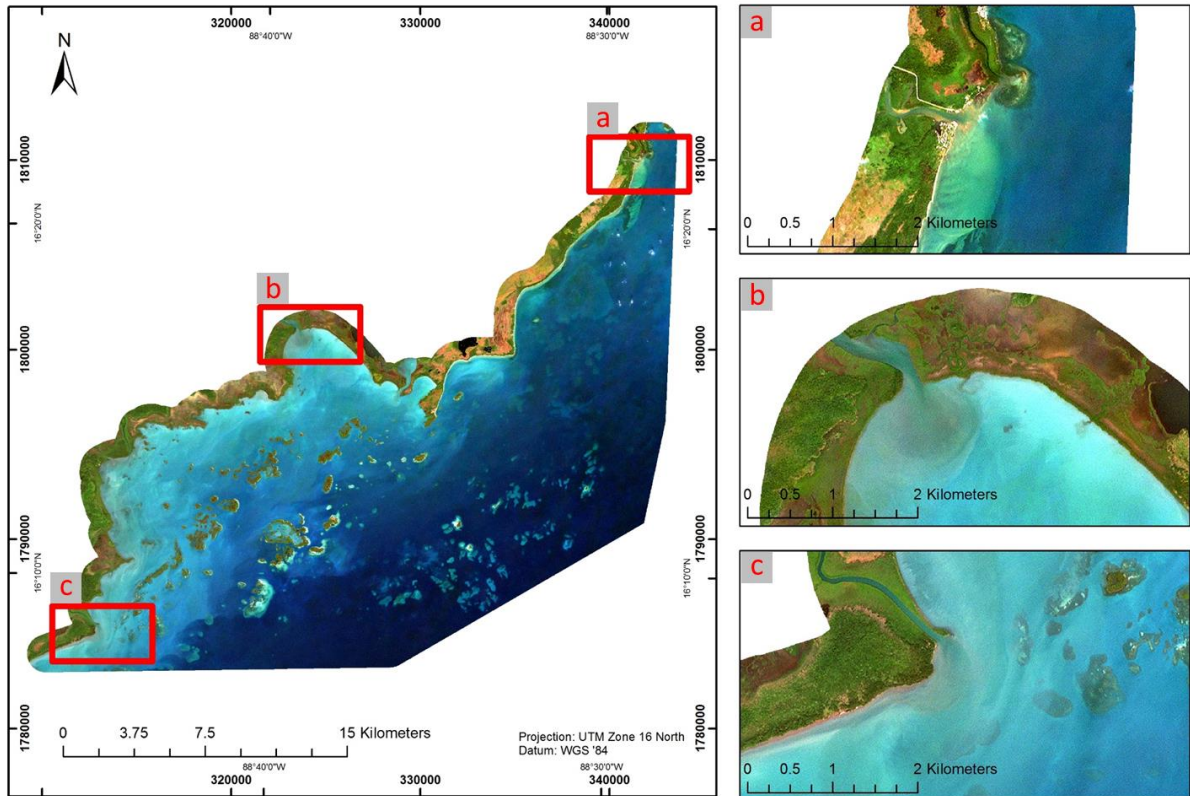


Figure 10: Examples for strong turbid sea within the project area. Here it was not possible to detect 4 density classes for seagrass. True-color RapidEye imagery (02/02/2016).

Figure 11 illustrates the hierarchical structure of the classification scheme, each ecological class is represented by the colours of the final maps (see Chapter 5).

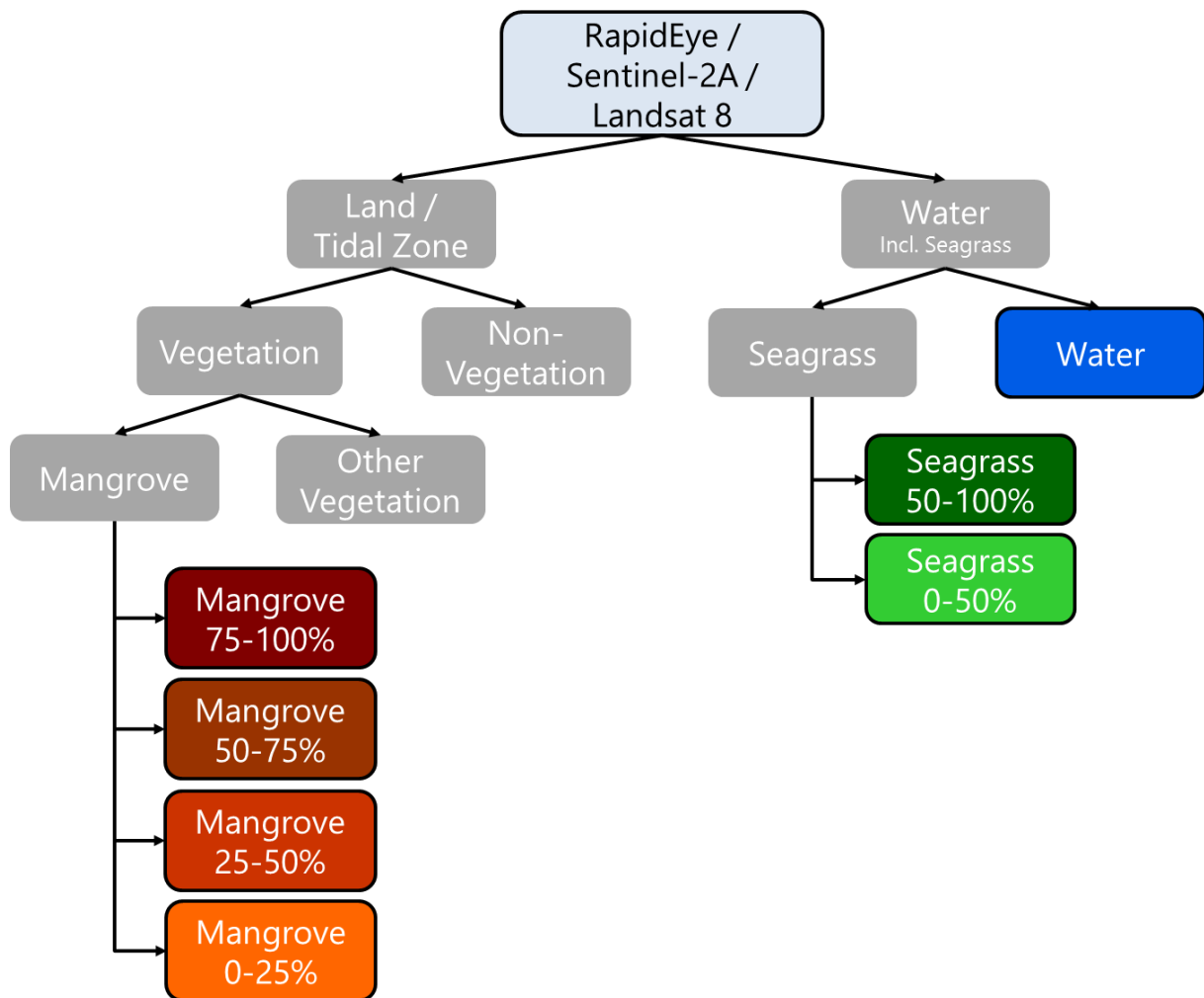


Figure 11: Classification scheme of the mangrove and seagrass cover classification of the Port Honduras Marine Reserve. Grey boxes without frame represent parent classes, framed boxes represent the final classes with the associated colour from the land cover maps (see Chapter 5).

The RapidEye image mosaic was segmented into objects of adjacent, spectrally similar pixels by the multi-resolution segmentation algorithm implemented in eCognition, and subsequently classified according to the classification scheme shown in Figure 11.

The classification rule-set works in a hierarchical manner from coarse to fine thematic details. On the first hierarchy level, discrimination between Land / Tidal Zone areas and Water areas (incl. seagrass) was conducted based on spectral thresholds.

On the next level of the hierarchy, all Land / Tidal Zone objects were discriminated into Vegetation and Non-Vegetation objects according to their spectral properties. Water was discriminated into Seagrass and Water.

On the third hierarchy level the vegetated objects were distinguished into Mangrove and Other Vegetation according to their spectral properties. Here also spectral properties from Sentinel-2A data were incorporated in the classification process as especially the shortwave infrared and near infrared bands have shown to be very helpful in differentiating mangroves from other vegetation (Figure 4).

Mangrove was further distinguished into 4 density classes (75-100%, 50-75%, 25-50%, and 20-25%) and seagrass into two density classes (50-100% and 0-50%) based on spectral and texture properties, as well as visual interpretation of the imagery.

After the object-oriented classification, an intensive visual revision by a trained expert was conducted. The results are georeferenced shp-files ready to be used in a geographic information system, like ArcGIS. XML-Metadata was generated for all deliverables.

Annex I gives an overview of the segmentation parameters, spectral bands, and spectral indices used. Further, the statistical parameters of the feature objects for the different classes are shown.

#### 4.4 Change Detection

Finally, to compare these up-to-date mangrove and seagrass maps (2016) with the ones derived for the year 2013 (Ballhorn et al. 2014) a post-classification change detection was conducted. In ArcGIS the resulting mangrove and seagrass maps of the two classifications (2013 and 2016) were intersected in order to derive areas of change. Figure 12 schematically displays the workflow of this post-classification change detection process. Our approach is a quantitative and qualitative comparison of two classifications (2013 and 2016).

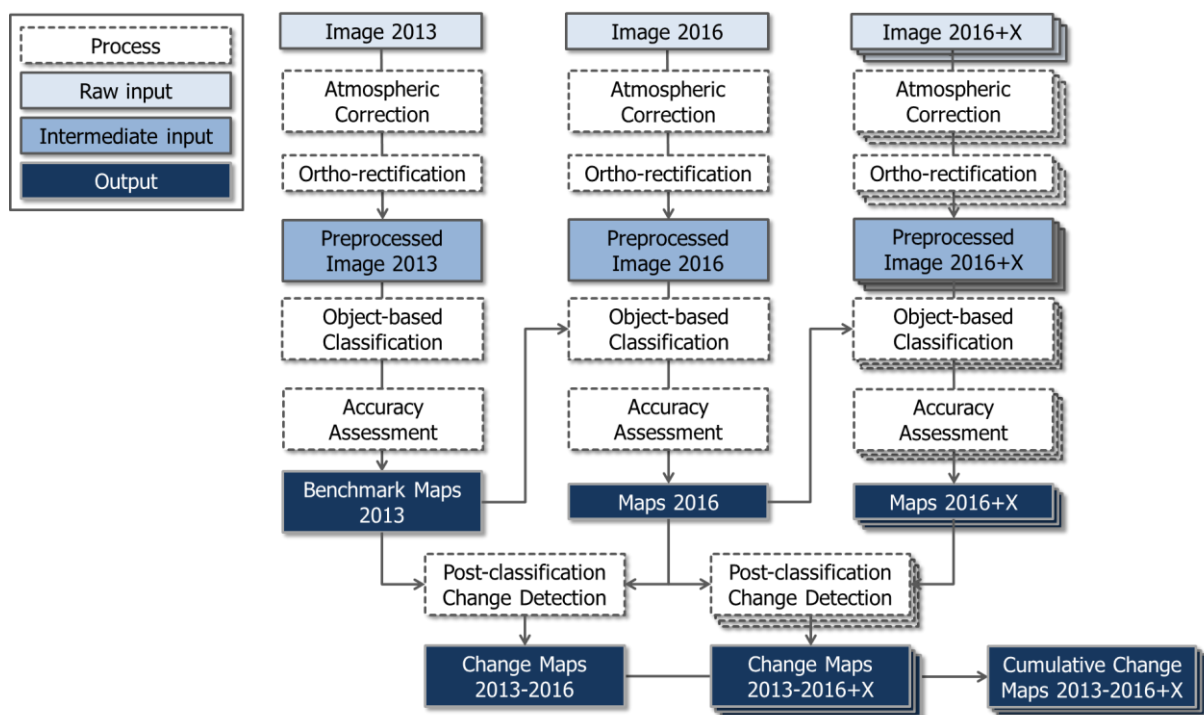


Figure 12: Schematic representation of the post-classification change detection process in order to analyse changes in mangrove and seagrass cover between the two classifications (2013, 2016). It also illustrates how future post-classification change detections would be conducted and implemented.

Monitoring techniques based on multispectral satellite-acquired data have demonstrated potential as a means to detect, identify, and map changes in forest cover (Coppin 2004) and seagrass (Misvari and Hashim 2016).

## 5. Results

Figure 13 and Figure 14 show the results for the mangrove and seagrass cover classification for the year 2013 (see Ballhorn et al. 2014). The overview maps are provided as high-resolution pdfs, that may be printed in A0 and displayed at an enlarged scale on a desktop computer.

Table 6 gives an overview of the remote sensing data used for the mangrove and seagrass classification of the year 2013. Images with different acquisition dates within the year 2013 were used to get a preferably cloud free coverage of the study area.

Table 6: Overview of remote sensing data used for the mangrove and seagrass classification of the year 2013.

Rapid Eye		
Amount tiles	Acquisition date	Cloud cover within study area (%)
4 (level 3A)	01/11/2013	0
Landsat 8		
Amount images	Acquisition date	Cloud cover within study area (%)
1	22/07/2013	1

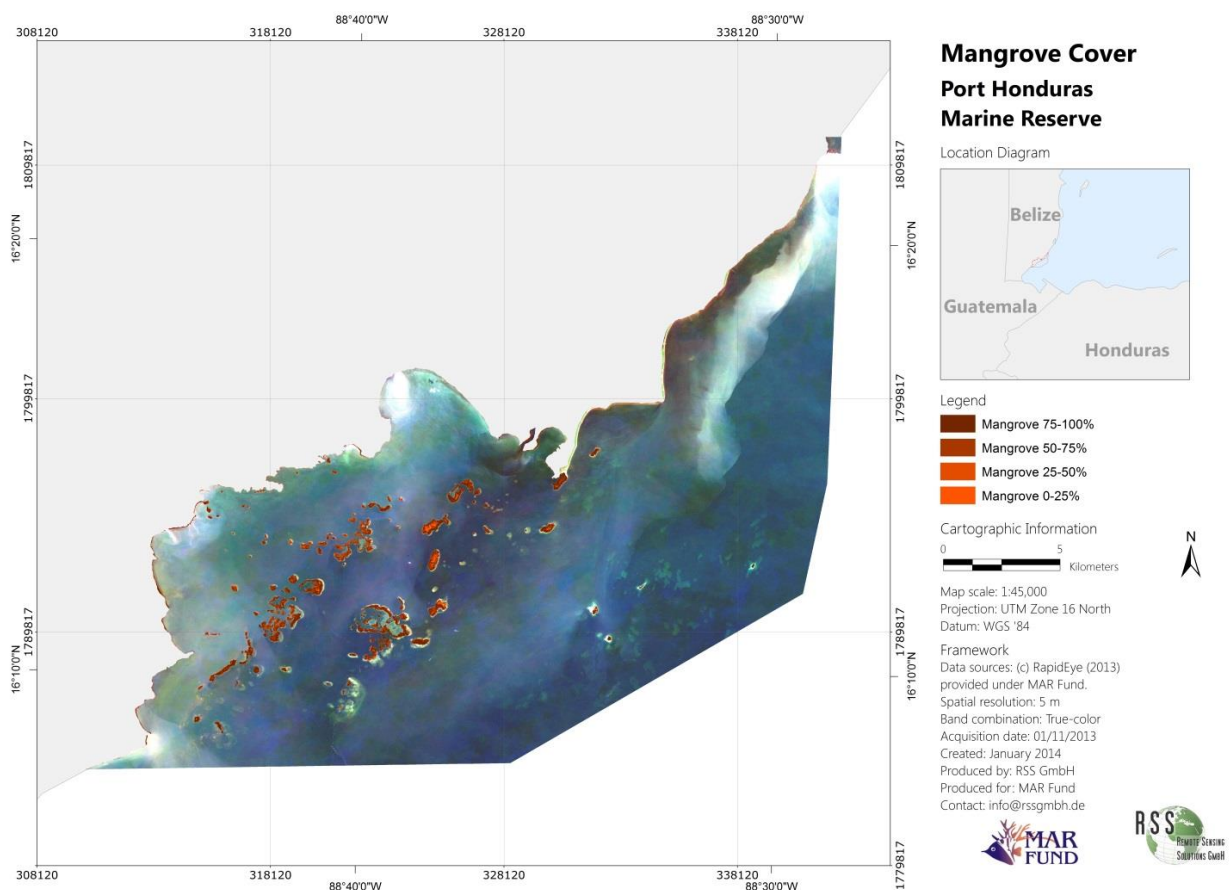


Figure 13: Mangrove cover classification for the Port Honduras Marine Reserve for the year 2013 (Ballhorn et al. 2014). Shown are the four mangrove density classes (0-25%, 25-50%, 50-75%, and 75-100%). In the upper right diagram the location of the Port Honduras Marine Reserve within Belize is displayed (red).

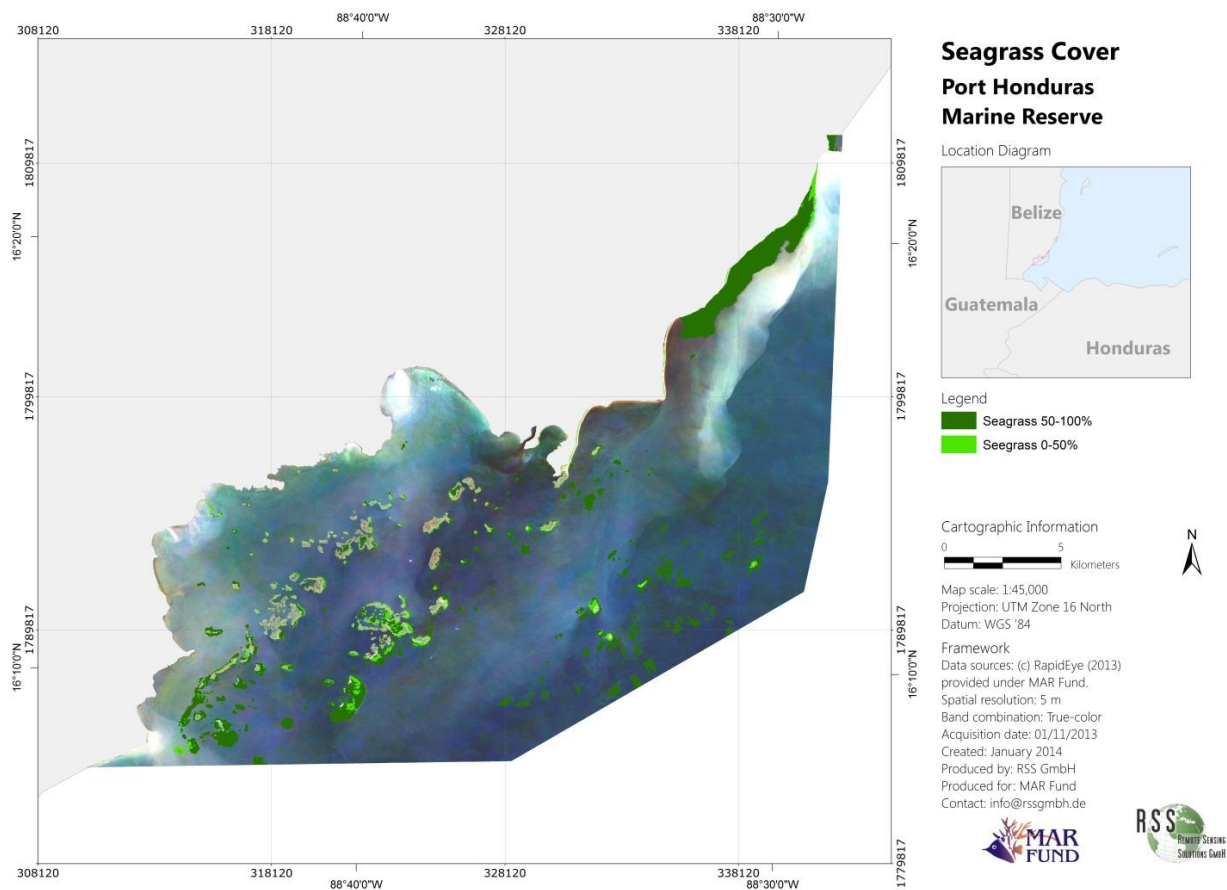


Figure 14: Seagrass cover classification for the Port Honduras Marine Reserve for the year 2013 (Ballhorn et al. 2014). Shown are the two seagrass density classes (0-50%, and 50-100%). In the upper right diagram the location of the Port Honduras Marine Reserve within Belize is displayed (red).

Table 7 displays the spatial extent of these different mangrove and seagrass classes for the year 2013 (see Ballhorn et al. 2014).

Table 7: Spatial extent of the different ecological classes classified for the year 2013 (Ballhorn et al. 2014) in the Port Honduras Marine Reserve. Also shown are the percentage of the total mangrove/seagrass cover and the percentage of the total Port Honduras Marine Reserve area for each class.

Year 2013			
Ecological Class	Area (ha)	Percentage of total mangrove/seagrass cover (%)	Percentage of total Port Honduras Marine Reserve (40,498.7 ha) (%)
Mangrove 75-100%	377	50	0.9
Mangrove 50-75%	238	31	0.6
Mangrove 25-50%	69	9	0.2
Mangrove 0-25%	73	10	0.2
<b>Sum Mangrove</b>	<b>757</b>	<b>100</b>	<b>1.9</b>
Seagrass 50-100%	2,084	89	5.1
Seagrass 0-50%	261	11	0.6
<b>Sum Seagrass</b>	<b>2,345</b>	<b>100</b>	<b>5.8</b>



Figure 15 and Figure 16 show the results for the mangrove and seagrass cover classification for the year 2016.

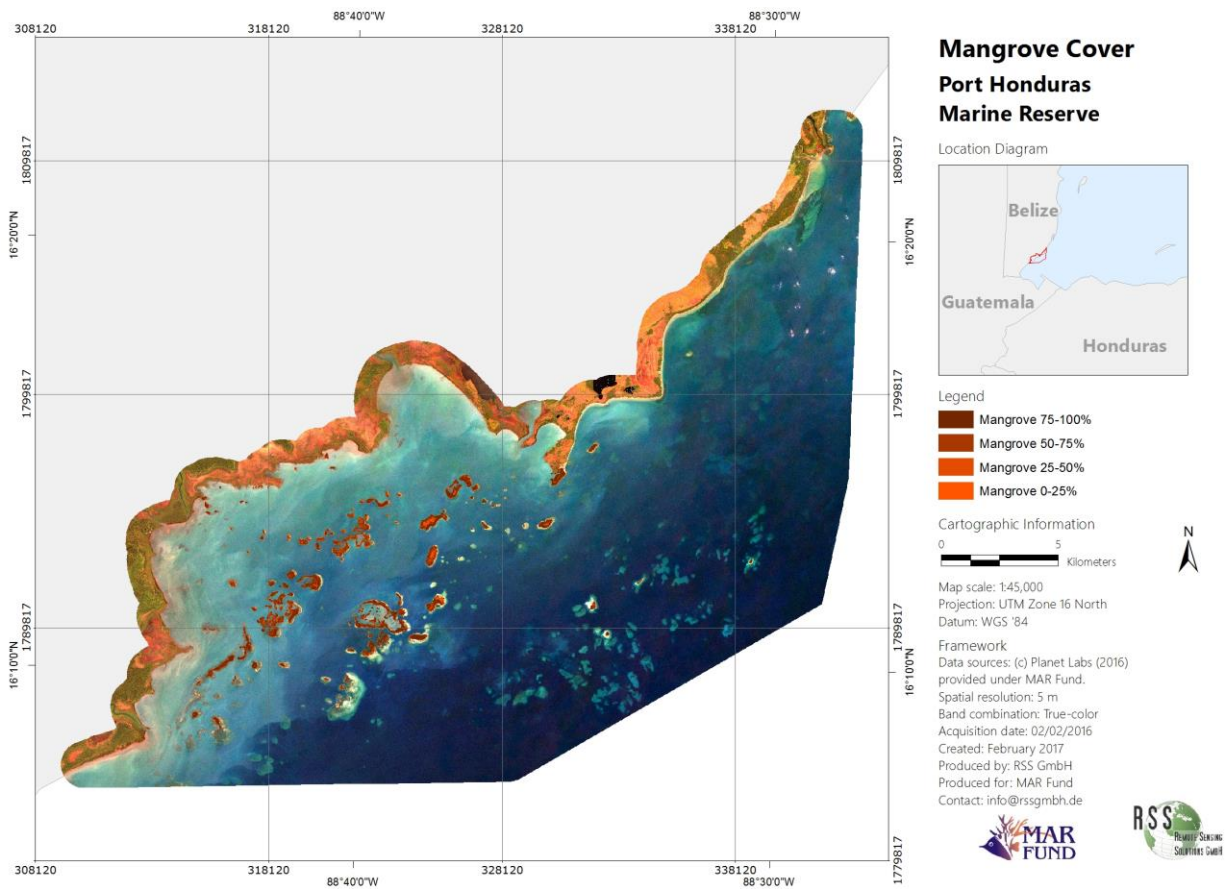


Figure 15: Mangrove cover classification for the Port Honduras Marine Reserve for the year 2016. Shown are the four mangrove density classes (0-25%, 25-50%, 50-75%, and 75-100%). In the upper right diagram the location of the Port Honduras Marine Reserve within Belize is displayed (red).

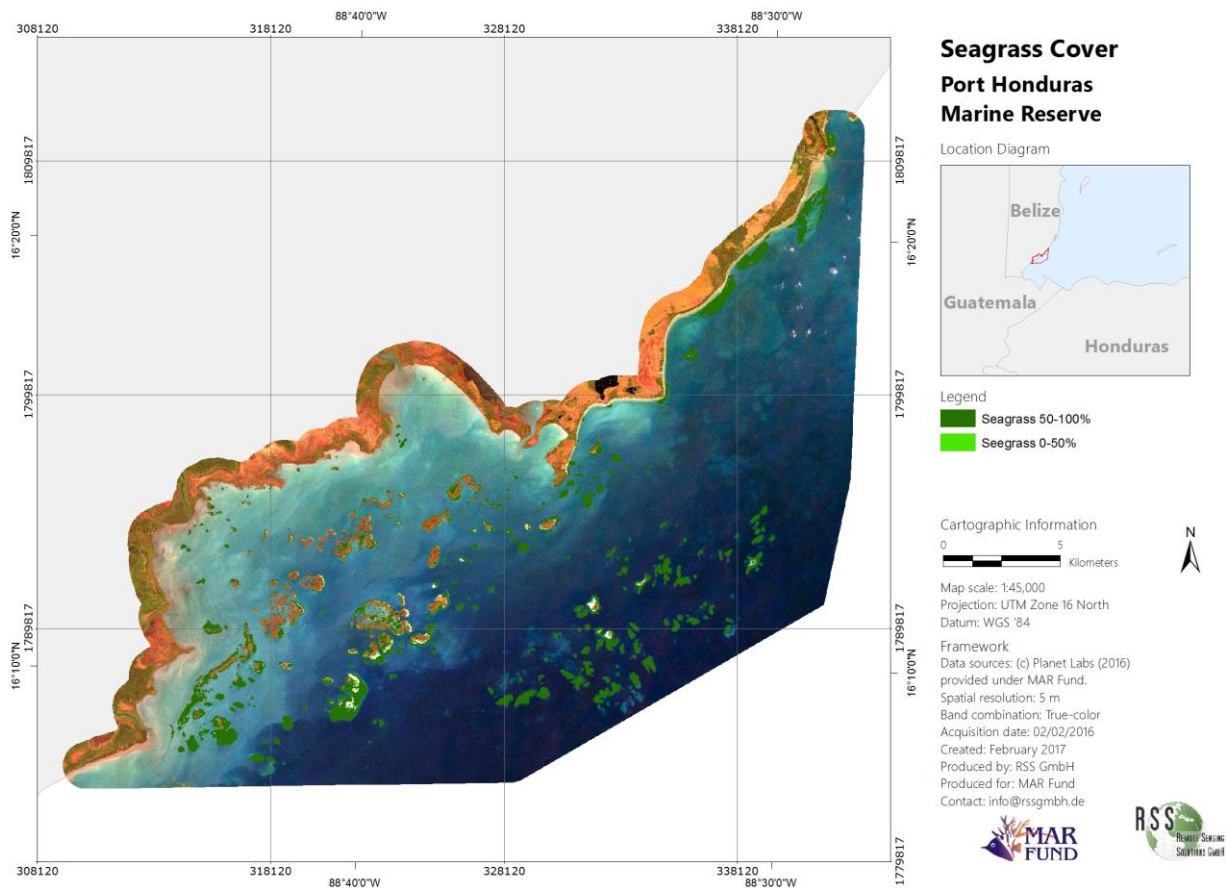


Figure 16: Seagrass cover classification for the Port Honduras Marine Reserve for the year 2016. Shown are the two seagrass density classes (0-50%, and 50-100%). In the upper right diagram the location of the Port Honduras Marine Reserve within Belize is displayed (red).

Table 8 displays the spatial extent of these different mangrove and seagrass classes for the year 2016.

Table 8: Spatial extent of the different ecological classes classified for the year 2016 in the Port Honduras Marine Reserve. Also shown are the percentage of the total mangrove/seagrass cover and the percentage of the total Port Honduras Marine Reserve area for each class.

Year 2016			
Ecological Class	Area (ha)	Percentage of total mangrove/seagrass cover (%)	Percentage of total Port Honduras Marine Reserve (40,498.7 ha) (%)
Mangrove 75-100%	382	50	0.9
Mangrove 50-75%	244	32	0.6
Mangrove 25-50%	61	8	0.2
Mangrove 0-25%	72	9	0.2
<b>Sum Mangrove</b>	<b>759</b>	<b>100</b>	<b>1.9</b>
Seagrass 50-100%	2,115	88	5.2
Seagrass 0-50%	292	12	0.7
<b>Sum Seagrass</b>	<b>2,408</b>	<b>100</b>	<b>5.9</b>

The graphs in Figure 17 and Figure 18 display the spatial extent of the different classes classified in the Port Honduras Marine Reserve for the year 2016. The colours represent the colours of each class in the final maps.

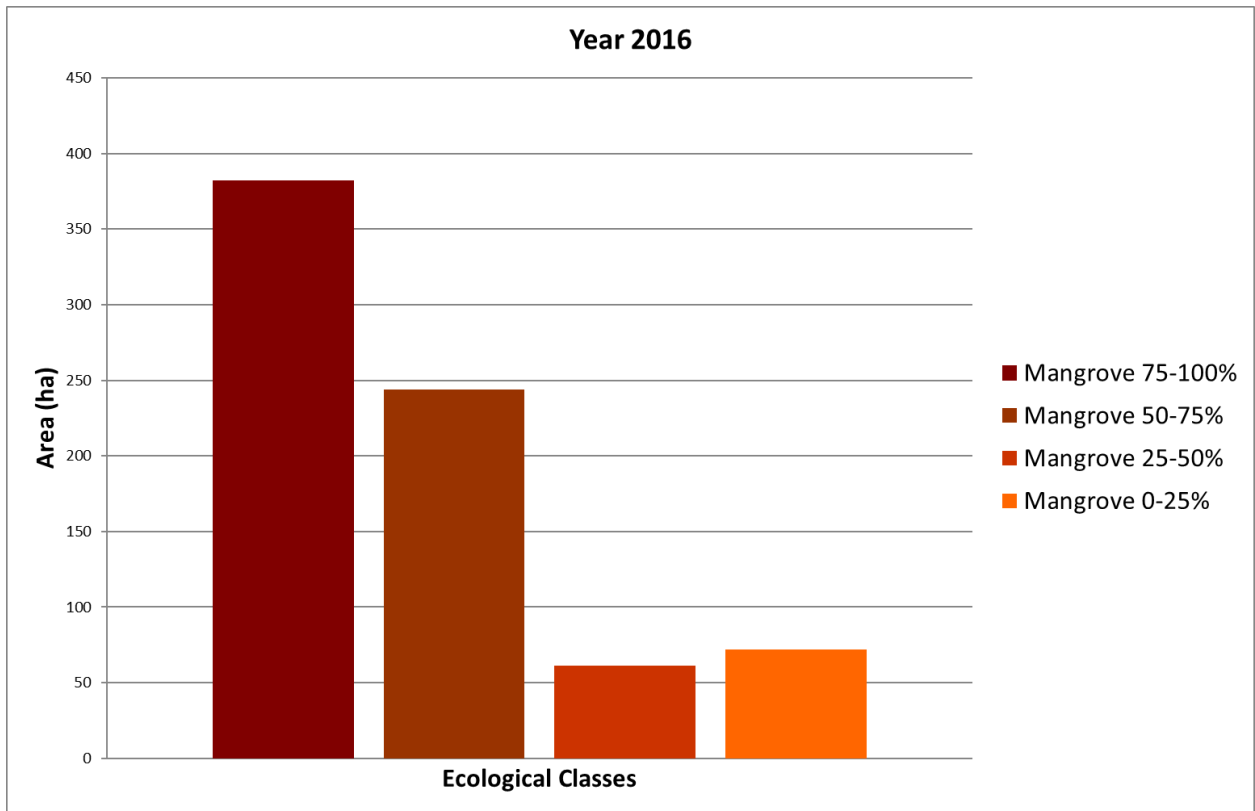


Figure 17: Spatial extent of the different mangrove density classes within the Port Honduras Marine Reserve for the year 2016. The colours represent the colours used in the land cover maps.

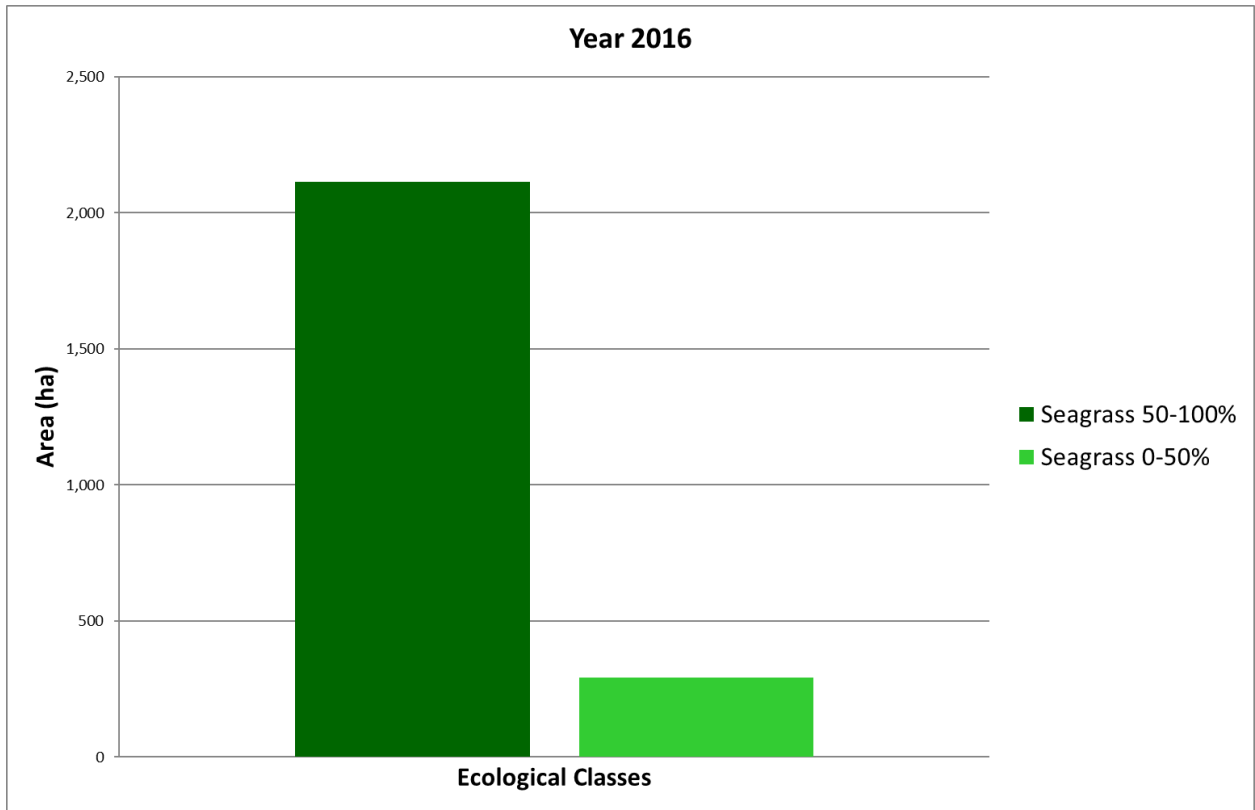


Figure 18: Spatial extent of the different seagrass density classes within the Port Honduras Marine Reserve for the year 2016. The colours represent the colours used in the land cover maps.

A detailed overview of the changes within the different classes between 2013 and 2016 is shown in Table 11.

Table 9: Detailed change matrix of the different land covers between 2013 and 2016 in hectare (ha). The different colors of the cells represent whether no change, loss, degradation or regeneration occurred within the mangrove or seagrass classes. The legend at the bottom of the table displays which color represents which change process.

		Classification 2016 (ha)								
		Land / Tidal Zone	Mangrove 0-25	Mangrove 25-50	Mangrove 50-75	Mangrove 75-100	Seagrass 0-50	Seagrass 50-100	Water	Sum
Classification 2013	Land / Tidal Zone	68.575	0.438	0.010	0.113	0.620		0.008	0.260	70.022
	Mangrove 0-25		70.957	0.055	1.912	0.450			0.020	73.395
	Mangrove 25-50		0.058	61.213	7.682	0.412				69.365
	Mangrove 50-75		0.028	0.003	231.205	6.395		0.025		237.655
	Mangrove 75-100		0.013	0.005	2.403	374.278				376.698
	Seagrass 0-50	0.007	0.407		0.300	0.083	200.555	22.975	36.618	260.945
	Seagrass 50-100	0.158	0.110		0.143		57.605	1,544.565	481.375	2,083.955
	Water	0.388	0.100				34.235	547.583	36,744.358	37,326.663
	Sum	69.127	72.110	61.285	243.757	382.238	292.395	2,115.155	37,262.630	40,498.697
	<b>No Change</b>									
	<b>Loss</b>									
	<b>Degradation</b>									
	<b>Gain</b>									
	<b>Regeneration</b>									

Table 10 summarizes these changes (2013 – 2016). Here deforestation is the change of one of the mangrove density classes to a non mangrove class and degradation is the change of one of the density classes (mangrove or seagrass) to a lower density class of the same land cover.

Table 10: Summarized changes (2013 – 2016) in hectare (ha). Mangrove reforestation and regeneration is clearly proven between 2013 and 2016, as well as seagrass gain and regeneration in the same time frame

<b>Change Class</b>	<b>Area (ha)</b>
Mangrove Deforestation	0.020
Mangrove Degradation	2.508
Mangrove Reforestation	1.280
Mangrove Regeneration	16.908
Seagrass Loss	518.158
Seagrass Degradation	57.605
Seagrass Gain	581.825
Seagrass Regeneration	22.975
Mangrove to Seagrass	0.025
Seagrass to Mangrove	1.042
Land / Tidal Zone to Water	0.260
Water to Land / Tidal Zone	0.388
No Change	39295.705

Following Table 10 mangrove reforestation / regeneration and seagrass gain / regeneration clearly indicate that MAR Fund's activities led to positive developments from 2013 to 2016. However, seagrass meadows are difficult to detect due to turbid waters and bad weather conditions, so that the statistics in Table 10 have to be carefully interpreted. The area gain / loss of seagrass meadows is rather explainable with different image data quality and varying turbidity levels between 2013 and 2016.

Figure 19 displays areas of land cover change between 2013 and 2016 within the Port Honduras Marine Reserve.



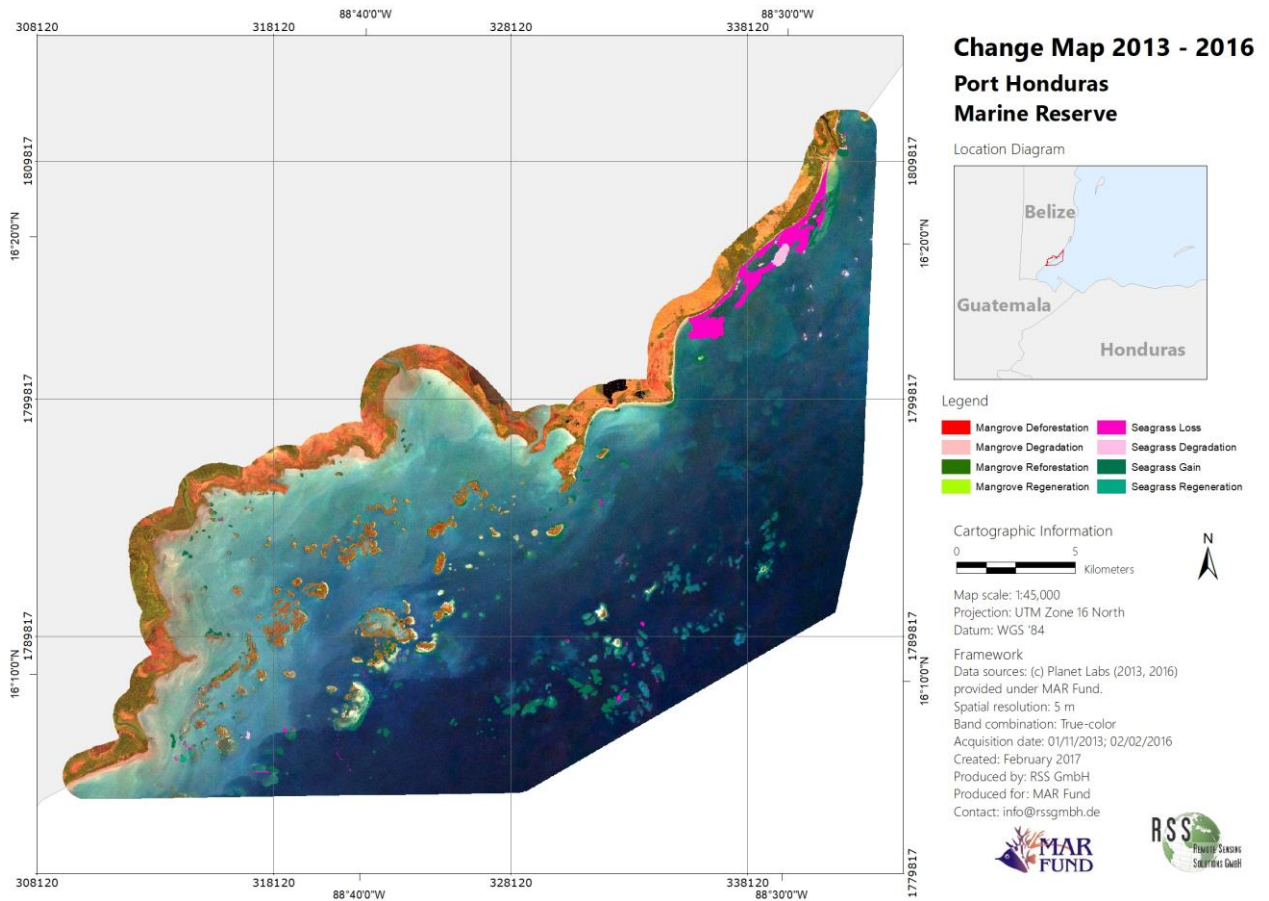


Figure 19: Land cover change map for the period between the years 2013 and 2016. In the upper right diagram the location of the Port Honduras Marine Reserve within Belize is displayed (red).

Figure 20 displays areas of change within the Port Honduras Marine Reserve in more detail.

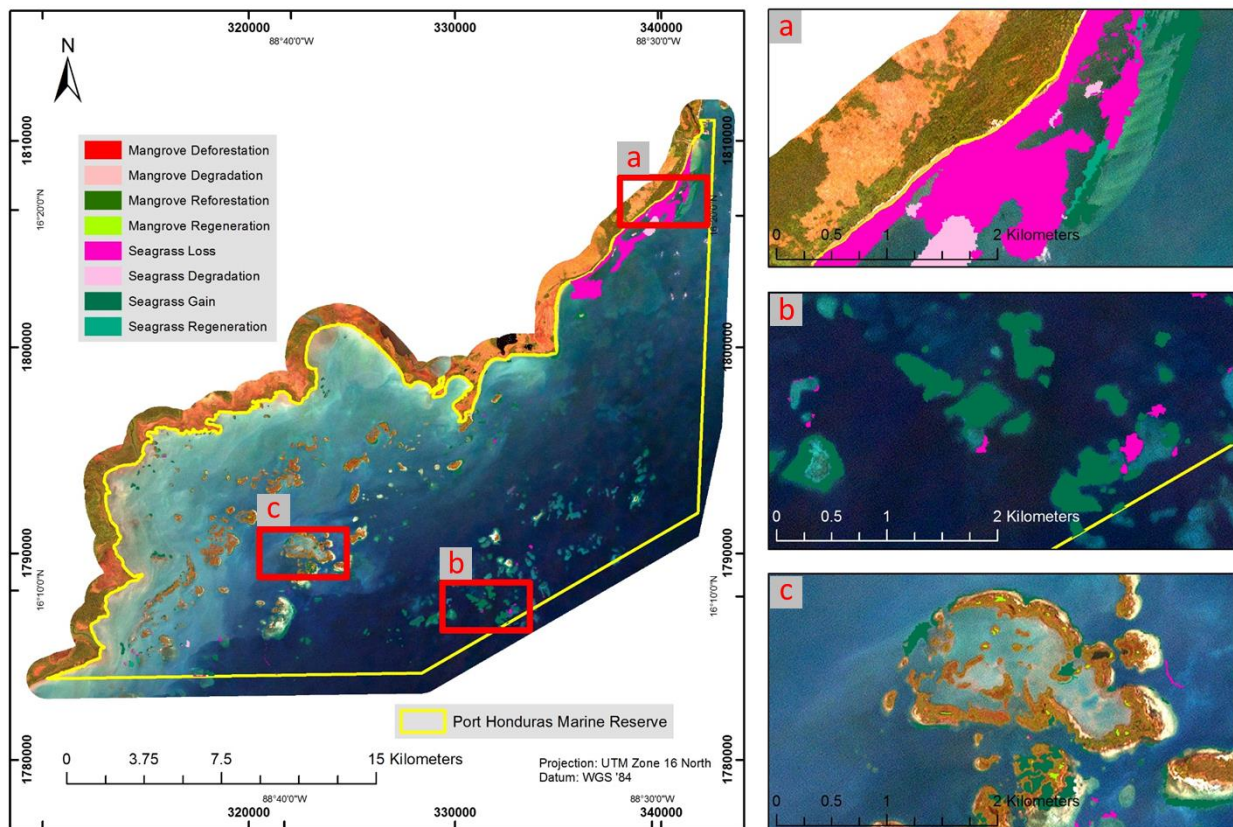


Figure 20: Examples for mangrove and seagrass changes detected between 2013 and 2016. The changes are superimposed on true-color RapidEye imagery (25/06/2016).

A seagrass area is identified as “Seagrass Degradation” (Figure 20 (a)). These coastal challow waters have high turbidity levels and have to be interpreted with caution. Here further ground truth data could help to minor uncertainty.

## 6. Accuracy Assessment

An independent accuracy assessment and verification of the classification results with reference data is an essential component. The accuracy analysis provides a confusion matrix considering user and producer accuracies, the overall accuracy and the kappa index (Congalton 1991). Regarding the amount of ground truth data for this accuracy assessment a balance between what is statistically sound and what is practicable must be found (Congalton and Green 1999). Congalton and Green (1999) propose as a “rule of thumb” to collect a minimum of 50 samples for each class in the error matrix. Ground truth data points were collected directly by local experts of the project partners at Port Honduras Marine Reserve. The ground truth campaign was planned in close cooperation with RSS GmbH. The field data assessment followed a strict protocol provided by RSS GmbH to assure objectivity and scientific validity. 40 ground truth sample points (20 marine and 20 terrestrial sample points) were collected in the field (Figure 21) by local experts in Belize between 06.-20.02.2017. Information collected in the field was recorded into different field sheets (one for marine and one for terrestrial sample points). In Annex II these two different field sheets are provided. Based on this information each collected in-situ sample point was allocated to one of the land cover classes.

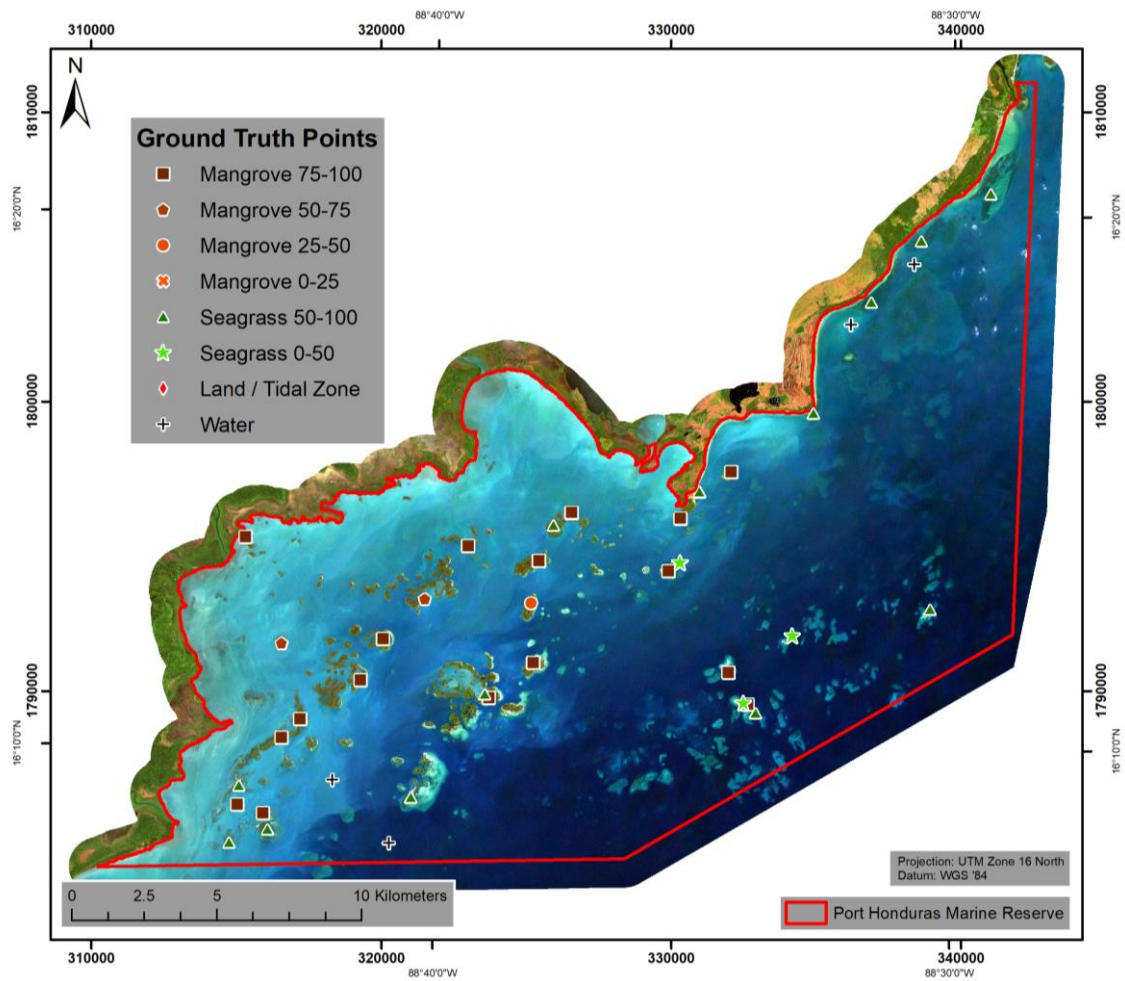


Figure 21: Location of the 40 ground truth data points collected by the local experts of the project partners at Port Honduras Marine Reserve.

The field data assessment was implemented by local experts at Port Honduras Marine Reserve. Figure 22 gives examples of this collected field data.



### Mangroves



Mangroves 0-25%



Mangroves 25-50%

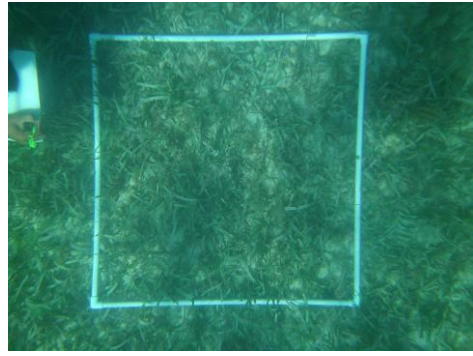


Mangroves 50-75%



Mangroves 75-100%

### Seagrass



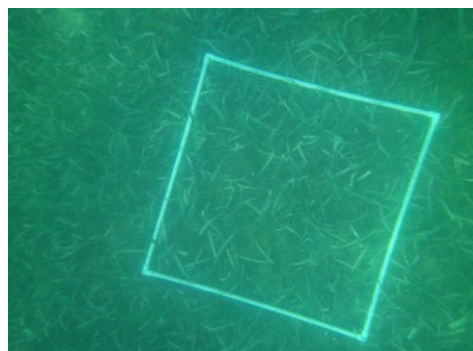
Seagrass 0-50%



Seagrass 50-100%



Seagrass 50-100%



Seagrass 50-100%

Figure 22: Examples of mangrove and seagrass density classes collection in the field by local experts. This data was used as input to the accuracy assessment.

As the ground truth data collection did not reach the sufficient amount of 50 points per class, additional samples of the original data (RapidEye imagery) were analyzed (Congalton and Green 1999). A random sample of additional 360 points was selected using ArcGIS, which were afterwards interpreted by an independent remote sensing expert not involved in the classification. Random sampling reduces the risk of bias and allows for an objective assessment of the uncertainty of the estimates. Table 11 shows the amount of samples per class collected in the field and the amount collected in the original satellite imagery (RapidEye).

Table 11: Amount of ground truth samples per class collected in the field and collected in the original RapidEye satellite imagery.

Class	Collected in the field	Collected in the imagery*	Sum
Mangrove 75-100%	17	33	50
Mangrove 50-75%	2	48	50
Mangrove 25-50%	1	49	50
Mangrove 0-25%	0	50	50
Seagrass 50-100%	13	37	50
Seagrass 0-50%	3	47	50
Land/Tidal Zone	0	50	50
Water	4	46	50
<b>Sum</b>	<b>40</b>	<b>360</b>	<b>400</b>

\* Original RapidEye satellite imagery

Several statistical measures for the accuracy (overall accuracy, Kappa coefficient's of agreement, producer's and user's accuracy per class) were calculated. Table 12 and Table 13 show the detailed results of the accuracy assessment. An **overall accuracy of 80.5%** with a **Kappa coefficient of 0.78** was realized.

Table 12: Confusion matrix per class by the use of 400 reference samples.

Confusion Matrix	Validation class								
	Mangrove 75-100%	Mangrove 50-75%	Mangrove 25-50%	Mangrove 0-25%	Seagrass 50-100%	Seagrass 0-50%	Land/Tidal Zone	Water	Sum
Mangrove 75-100%	29	15	5				1		50
Mangrove 50-75%		26	23	1					50
Mangrove 25-50%			39	10		1			50
Mangrove 0-25%			4	46					50
Seagrass 50-100%					37	10		3	50
Seagrass 0-50%					2	46		2	50
Land/Tidal Zone							50		50
Water					1			49	50
Sum	29	41	71	57	40	57	51	54	400



Table 13: Producer's and User's Accuracy per class.

<b>Class</b>	<b>Producer's Accuracy</b>	<b>User's Accuracy</b>
<b>Mangrove 75-100%</b>	100.0%	58.0%
<b>Mangrove 50-75%</b>	63.4%	52.0%
<b>Mangrove 25-50%</b>	54.9%	78.0%
<b>Mangrove 0-25%</b>	80.7%	92.0%
<b>Seagrass 50-100%</b>	92.5%	74.0%
<b>Seagrass 0-50%</b>	80.7%	92.0%
<b>Land/Tidal Zone</b>	98.0%	100.0%
<b>Water*</b>	90.7%	98.0%

## 7. Deliverables

- Original RapidEye imagery from 02/02/2016 (GeoTIFF)
- Original Sentinel-2A imagery from 11/03/2016 (JPEG 2000)
- Original Landsat 8 image from 31/08/2016 (GeoTIFF)
- Preprocessed RapidEye image mosaic from 02/02/2016 (Band Sequential (.bsq) image file), XML-Metadata
- Preprocessed Sentinel-2A image from 11/03/2013 (GeoTIFF), XML-Metadata
- Preprocessed Landsat 8 image from 31/08/2016 (Band Sequential (.bsq) image file), XML-Metadata
- Mangrove cover classification (Shapefile and Layerfile), XML-Metadata
- Seagrass cover classification (Shapefile and Layerfile), XML-Metadata
- Change 2013 – 2016 (Shapefile and Layerfile), XML-Metadata
- Mangrove map in A0 (pdf and ArcGIS .mxd-file), XML-Metadata
- Seagrass map in A0 (pdf and ArcGIS .mxd-file), XML-Metadata
- Change Map in A0 (pdf and ArcGIS .mxd-file), XML-Metadata

## Conclusions

This study has shown that seagrass and mangrove coverage can be reliably assessed using actual high-resolution satellite imagery in good quality at low costs.

Two main objective indicators of the MAR Fund have been accomplished at the end of the project:

- Areas of mangrove in project MCPA 2016 are equal to or greater than the baseline (as assessed in 2013)
- Areas of marine seagrass beds in project MCPA 2016 are equal to or greater than the baseline (as assessed in 2013)

The ground truth campaign implemented by local experts provides an excellent basis for a realistic accuracy assessment and confirms the results of this study. To improve the outcome of the accuracy assessment activities in future projects, it should be planned to extent local ground truth activities (also within the project budget considerations). At least 50 samples for each desired class should be collected (Congalton and Green 1999). For areas larger than 400,00 ha at least 75 samples should be collected per desired class (Congalton and Green 1999).

The results of this study show that MAR Fund's activities on conservation and restoration from 2013 to 2016 have proven to be present and verifiable as displayed in Table 10.

## References

- Atkinson, P. M. and Lewis, P. (2000). Geostatistical classification for remote sensing: an introduction. *Computer & Geosciences*, Volume 26, pp.361-371.
- Ballhorn, U., Mott, C., Siegert, F. (2014). Establishing the baseline for seagrass and mangrove area cover in four Marine and Coastal Priority Protected Areas within the Meso-American Reef area. Port Honduras Marine Reserve, Belize. Final report, MAR Fund.
- Benz, U. C., Hofmann, P., Wilhauk, G., Lingenfelder, I., Heyen, M. (2004). Multi-resolution, object-oriented fuzzy analysis of remote sensing data for GIS-ready information. *Isprs J Photogramm* 58 (3-4), pp. 239-258.
- Chen, C. F., Son, N. T., Chang, N. B., Chen, C. R., Chang, L. Y., Valdez, M., Centeno, G., Thompson, C. A., Aceituno, J. L. (2013). Multi-Decadal Mangrove Forest Change Detection and Prediction in Honduras, Central America, with Landsat Imagery and a Markov Chain Model. *Remote Sensing*, Volume 5, pp.6408-6426.
- Cherrington, E. A. (2013). Baseline Assessment of Seagrass and Mangrove Cover and Dynamics in the Port Honduras Marine Reserve, Belize. Technical Report, Water Center for the Humid Tropics of Latin America & the Caribbean (CATHALAC), Panama City, Panama.
- Congalton, R.G. (1991). A Review of Assessing the Accuracy of Classifications of Remotely Sensed Data. *Remote Sens Environ* 37(1), pp. 35-46.
- Congalton, R.G. and Green, K. (1999). *Assessing the Accuracy of Remotely Sensed Data: Principles and Practices*. CRC Press, Inc., United States of America.
- Coppin P., Jonkheree, I., Nackarts, K., Muys, B., Lambin, E. (2004): Digital change detection methods in ecosystem monitoring: a review. *Int J Remote Sens* 25(9), S.1565-1596.
- Dekker, A., Brando, V., Anstee, J., Fyfe, S., Malthus, T., Karpouzli, E. (2006). Remote Sensing of Seagrass Ecosystems: Use of Spaceborne and Airborne Sensors. *Seagrasses: Biology, Ecology and Conservation 2006*, pp. 347-359.
- Giri, C., Ochieng, E., Tieszen, L. I., Shu, Z., Singh, A., Loveland, T., Duke N. (2011). Status and distribution of mangrove forests of the world using earth observation satellite data. *Global Ecol Biogeogr*. Volume 20, pp. 154–159.
- Green, E. P., Mumby, P. J., Edwards, A. J., Clark, C. D. edited by Edwards, A. J. (2004). *Remote Sensing Handbook for Tropical Coastal Management*.
- Guindon, B. (1997). Computer-Based Aerial Image Understanding: A Review and Assessment of its Applications to Planimetric Information Extraction from Very High Resolution Satellite Images. *Canadian Journal of Remote Sensing*, Volume 23, pp.38-47.
- Guindon, B. (2000). Combining Diverse Spectral, Spatial and Contextual Attributes in Segment-Based Image Classification. *ASPRS 2000 Annual Conference*.
- Haralick, R. M. and Joo, H. (1986). A Context Classifier. *IEEE Transactions on Geoscience and Remote Sensing*, Volume 24, pp.997-1007.
- Hay, G. J., Niemann, K. O., McLean, G. F. (1996). An object-specific image texture analysis of H-resolution forest imagery. *Remote Sensing of Environment*, Volume 55, pp.108-122.
- Kartikayan, B., Majumder, K. L., Dasgupta, A. R. (1995). An Expert-System for Land-Cover Classification. *IEEE Transactions on Geoscience and Remote Sensing*, Volume 33, pp.58-66.

- Kartikeyan, B., Sarkar, A., Majumder, K. L. (1998). A segmentation approach to classification of remote sensing imagery. *International Journal of Remote Sensing*, Volume 19, pp.1695-1709.
- Kettig, R. L. and Landgrebe, D. A. (1976). Classification of Multispectral Image Data by Extraction and Classification of Homogeneous Objects. *IEEE Transactions on Geoscience and Remote Sensing*, Volume 14, pp.19-26.
- Kuenzer, C., Bluemel, A., Gebhardt, S., Quoc, T.V., Dech, S. (2011). Remote Sensing of Mangrove Ecosystems: A Review. *Remote Sens.*, 3, pp. 878-928.
- Matsuyama, T. (1987). Knowledge-Based Aerial Image Understanding Systems and Expert Systems for Image-Processing. *IEEE Transactions on Geoscience and Remote Sensing*, Volume 25, pp.305-316.
- McField, M. and Kramer P. R. (Eds.) (2007). *Healthy Reefs for Healthy People: A Guide to Indicators of Reef Health and Social Well-being in the Mesoamerican Reef Region*. Smithsonian Institution. Available online: <http://www.healthyreefs.org/cms/publications/>.
- Misvari, S. and Hashim, M. (2016). Change Detection of Submerged Seagrass Biomass in Shallow Coastal Water. *Remote Sens.*, 8, 200; doi:10.3390/rs8030200.
- Mott, C (2005). *Objektorientierte Klassifikationsstrategien zur Erfassung der Landnutzung aus hochauflösenden Fernerkundungsdaten*. Technische Universität München. PhD-Thesis.
- Mumby, P. J., Green, E. P., Edwards, A. J., Clark. C. D. (1997). Coral reef habitat mapping: how much detail can remote sensing provide? *Marine Biology*. Volume 130, Issue 2, pp.193-202.
- Mumby, P.J., Green, E.P., Edwards, A.J. and Clark, C.D. (1999). The cost-effectiveness of remote sensing for tropical coastal resources assessment and management. *Journal of Environmental Management*, 55, pp.157-166.
- Richter, R. and Schläpfer, D. (2011). *Atmospheric / Topographic Correction for Satellite Imagery*. DLR report DLR-IB 565-02/11, Wessling, Germany, 202 pp.
- USGS website assessed in Feb. 2017. <http://landsat.usgs.gov/landsat8.php>.
- Wabnitz, C. C. C., Andrefouet, S., Torres-Pulliza, D., Muller-Karger, F. E., Kramer P. A. (2007). *Regional-scale seagrass habitat mapping in the Wider Caribbean Region using Landsat sensors: Applications to Conservation and Ecology*. University of British Columbia Fisheries Centre Working Paper Series. Working Paper # 2007-04. 44 pp.
- Woodcock, C. E., Strahler, A. H., Jupp, D. L. B. (1988). The use of variograms in remote sensing I: Scene models and simulated images. *Remote Sensing of Environment*, Volume 25, pp.323-348.

## Annex I

### List of Abbreviations for the different spectral bands and indices used

Abbreviation	Band/Description	Spectral Range/Central Wavelength (nm) or Equation
RE_blue	RapidEye 2016 blue	440-510
RE_green	RapidEye 2016 green	520-590
RE_red	RapidEye 2016 red	630-685
RE_red_edge	RapidEye 2016 red edge	690-730
RE_nir	RapidEye 2016 near infrared	760-850
SE2_B2	Sentinel-2A Band 2 blue	490
SE2_B3	Sentinel-2A Band 3 green	560
SE2_B4	Sentinel-2A Band 4 red	665
SE2_B5	Sentinel-2A Band 5 vegetation red edge	705
SE2_B6	Sentinel-2A Band 6 vegetation red edge	740
SE2_B7	Sentinel-2A Band 7 vegetation red edge	783
SE2_B8	Sentinel-2A Band 8 near infrared	842
SE2_B8a	Sentinel-2A Band 8a vegetation red edge	865
SE2_B11	Sentinel-2A Band 11 short wavelength infrared	1,610
SE2_B12	Sentinel-2A Band 12 short wavelength infrared	2,190
RE2013_blue	RapidEye 2016 blue	440-510
RE2013_green	RapidEye 2016 green	520-590
RE2013_red	RapidEye 2016 red	630-685
RE2013_red_edge	RapidEye 2016 red edge	690-730
RE2013_nir	RapidEye 2016 near infrared	760-850
Anthocyanin_RI	RapidEye Anthocyanin Reflectance Index	$(1/[Mean\ RE\_green]) / (1/[Mean\ RE\_red\_edge])$
Chlorophyll_Green	RapidEye Chlorophyll Green Index	$1 / ([Mean\ RE\_nir] / [Mean\ RE\_green])$
Cust_Brightness_RGB	RapidEye Cust Brightness RGB Index	$([Mean\ RE\_blue] + [Mean\ RE\_green] + [Mean\ RE\_red]) / 3$
Green_Ratio	RapidEye Green Ration Index	$([Mean\ RE\_green] + [Mean\ RE\_blue]) / [Mean\ RE\_blue]$
NDVI	RapidEye Normalized Difference Vegetation Index	$([Mean\ RE\_nir] - [Mean\ RE\_red]) / ([Mean\ RE\_nir] + [Mean\ RE\_red])$
NDWI_IR	RapidEye Normalized Difference Water Infrared Index	$([Mean\ RE\_green] - [Mean\ RE\_nir]) / ([Mean\ RE\_green] + [Mean\ RE\_nir])$
NDWI_Red_Edge	RapidEye Normalized Difference Water Red Edge Index	$([Mean\ RE\_green] - [Mean\ RE\_red\_edge]) / ([Mean\ RE\_green] + [Mean\ RE\_red\_edge])$



## Segmentation parameters used

Edit Process ? X

**Name**

Automatic

15 [shape:0.5 compct.:0.5] creating 'L1'

**Algorithm**

multiresolution segmentation

**Domain**

pixel level

Parameter	Value
Condition	---
Map	From Parent

**Loops & Cycles**

Loop while something changes only

Number of cycles: 1

**Algorithm Description**

Apply an optimization procedure which locally minimizes the average heterogeneity of image objects for a given resolution.

**Algorithm parameters**

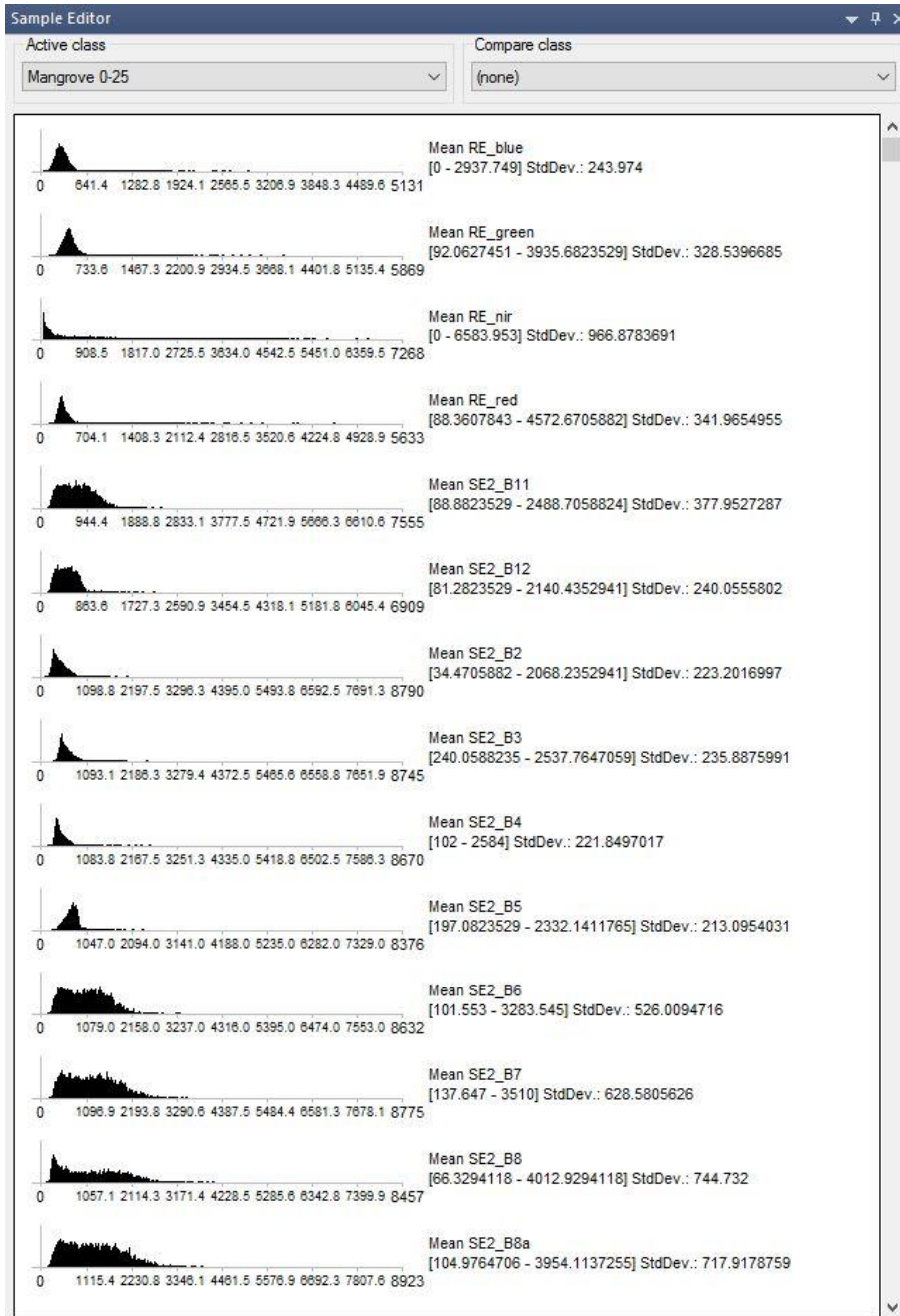
Parameter	Value
Overwrite existing level	Yes
<b>Level Settings</b>	
Level Name	L1
Compatibility mode	None
<b>Segmentation Settings</b>	
Image Layer weights	0, 0, 0, 0, 0, 1, 1, 1, 1, 1, 1, 0, 0, 0, 0, 0, 0, 0, 0, 0
RE2013_blue	0
RE2013_green	0
RE2013_nir	0
RE2013_red	0
RE2013_red_edge	0
RE_blue	1
RE_green	1
RE_nir	1
RE_red	1
RE_red_edge	1
SE2_B11	0
SE2_B12	0
SE2_B2	0
SE2_B3	0
SE2_B4	0
SE2_B5	0
SE2_B6	0
SE2_B7	0
SE2_B8	0
SE2_B8a	0
<b>Thematic Layer usage</b>	
classification_2013	Yes
study_area	Yes
Scale parameter	15
<b>Composition of homogeneity criterion</b>	
Shape	0.5
Compactness	0.5

**Thematic Layer usage**

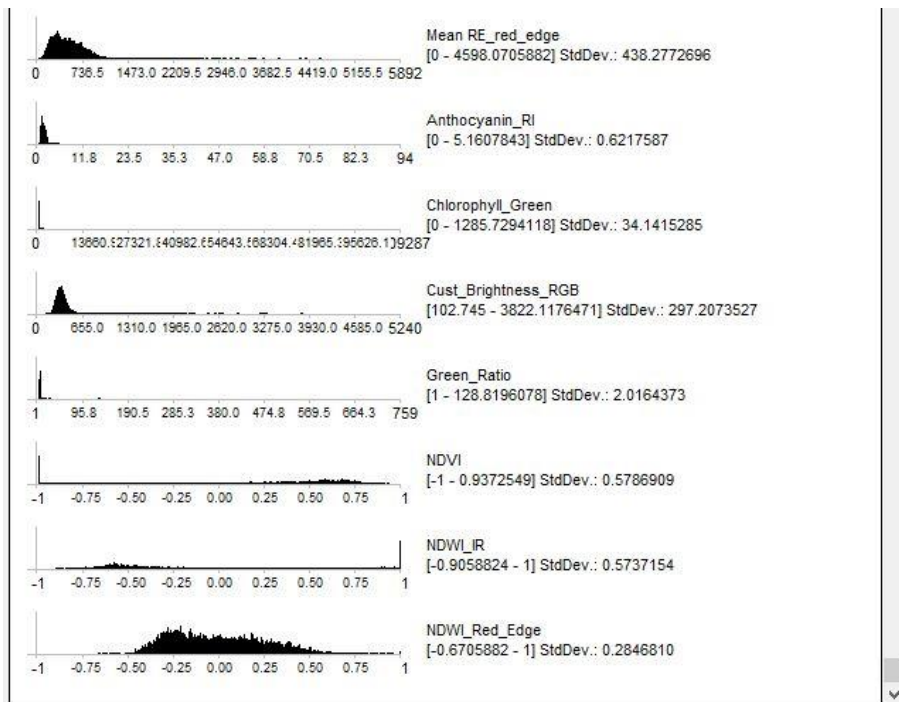
Thematic Layer usage flags

Execute Ok Cancel Help

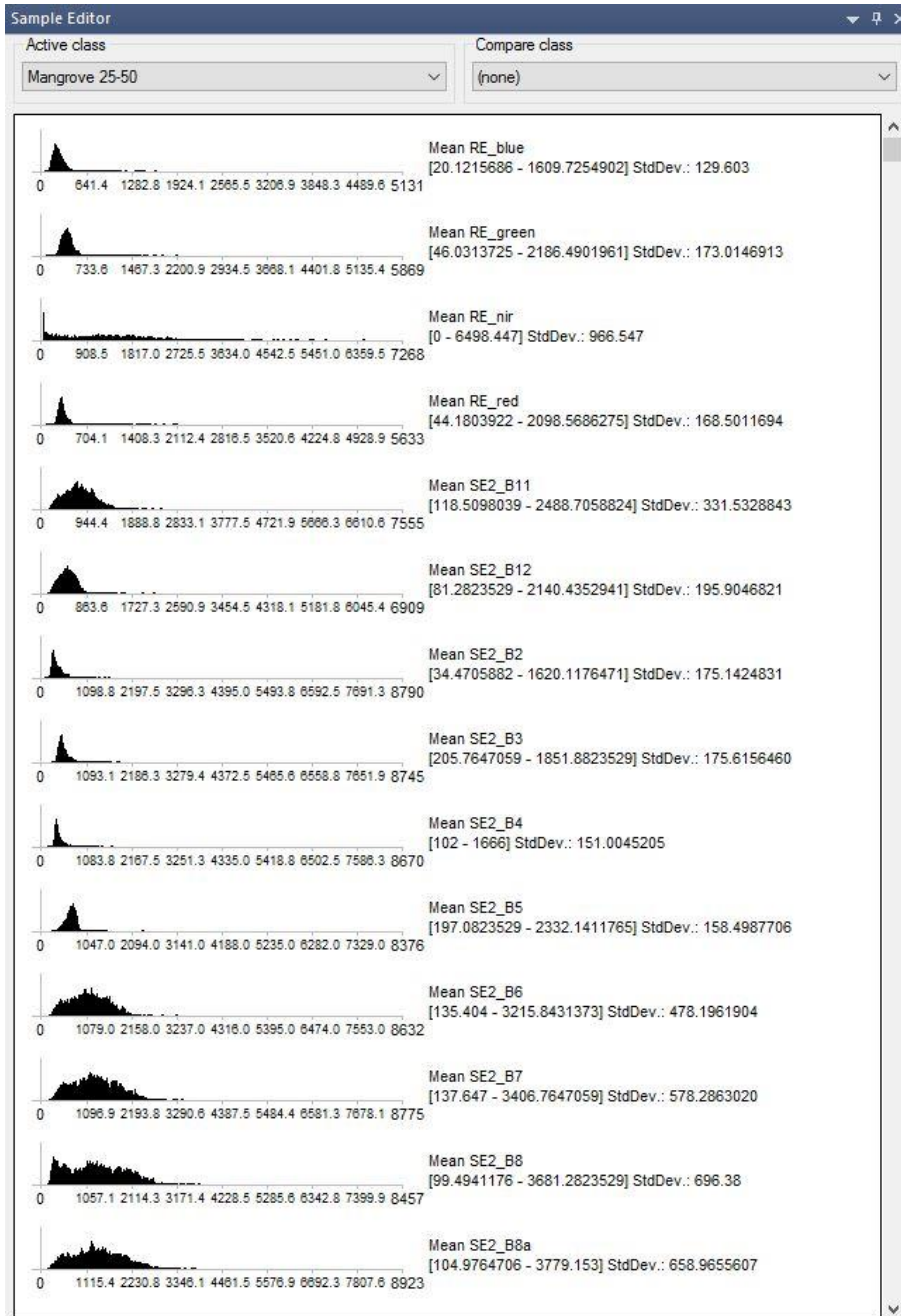
## Statistical parameters of the feature objects for the class Mangrove 0-25%



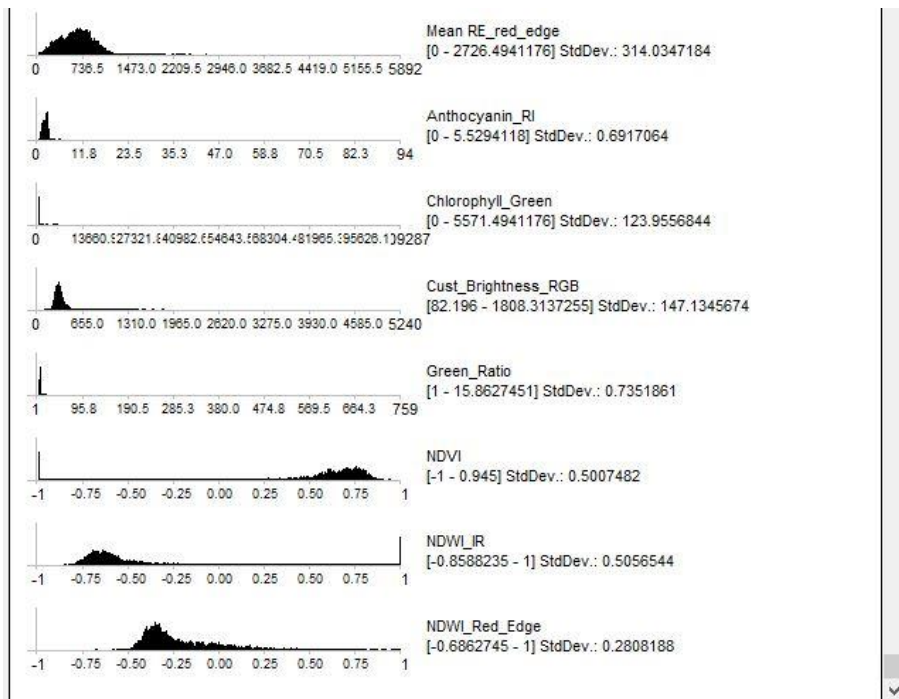
## Statistical parameters of the feature objects for the class Mangrove 0-25% cont.



## Statistical parameters of the feature objects for the class Mangrove 25-50%

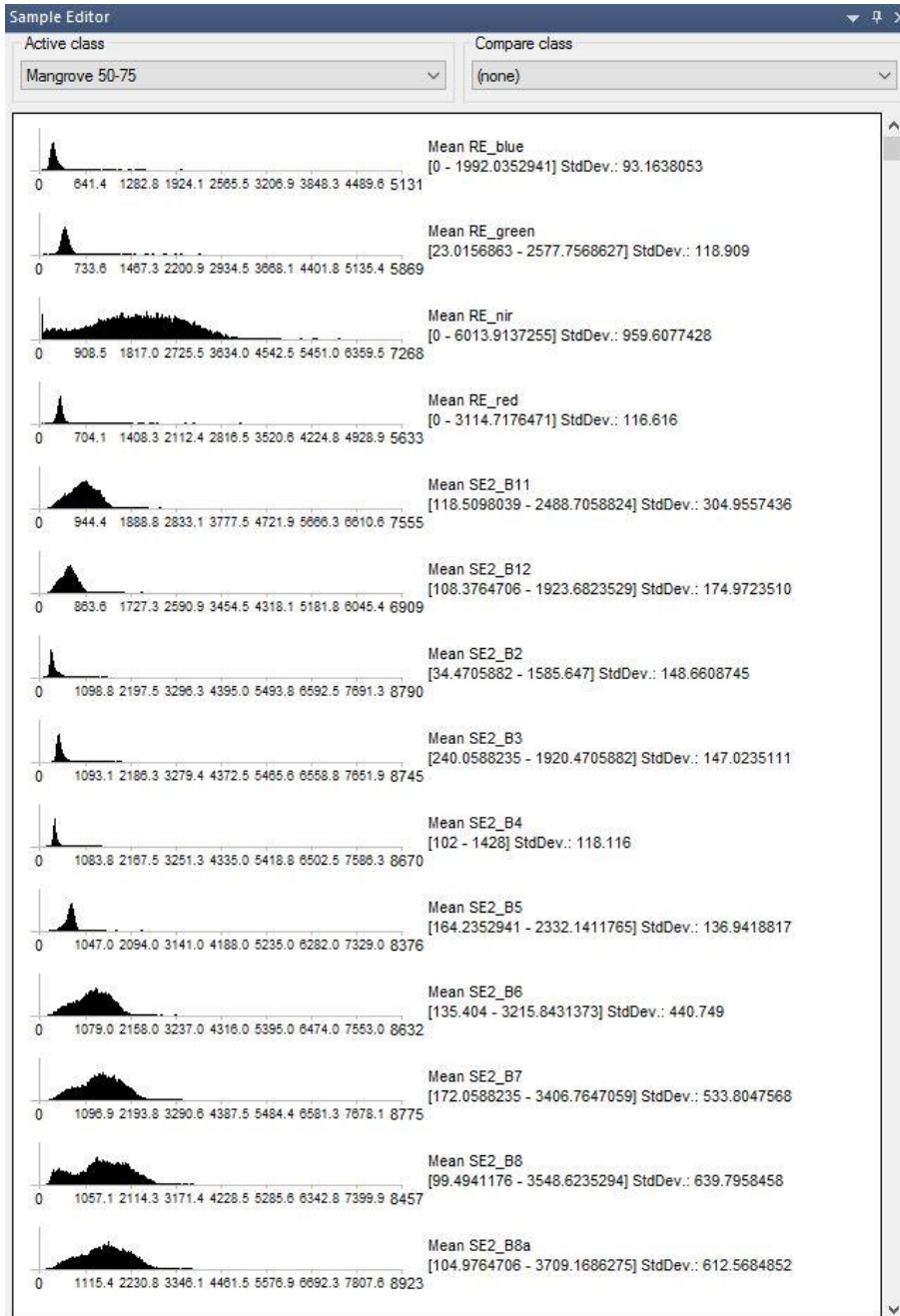


## Statistical parameters of the feature objects for the class Mangrove 25-50% cont.

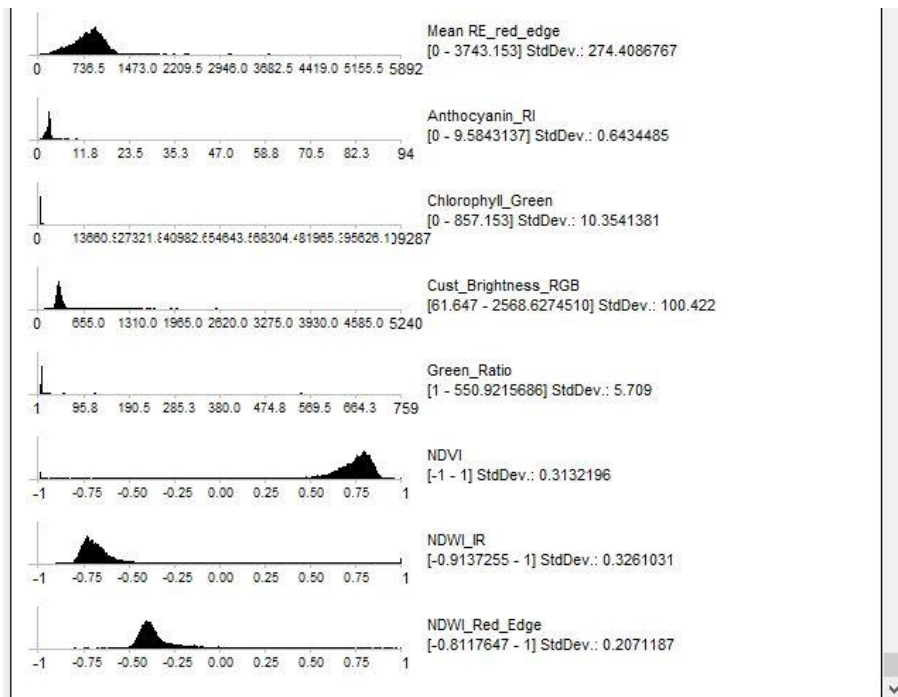




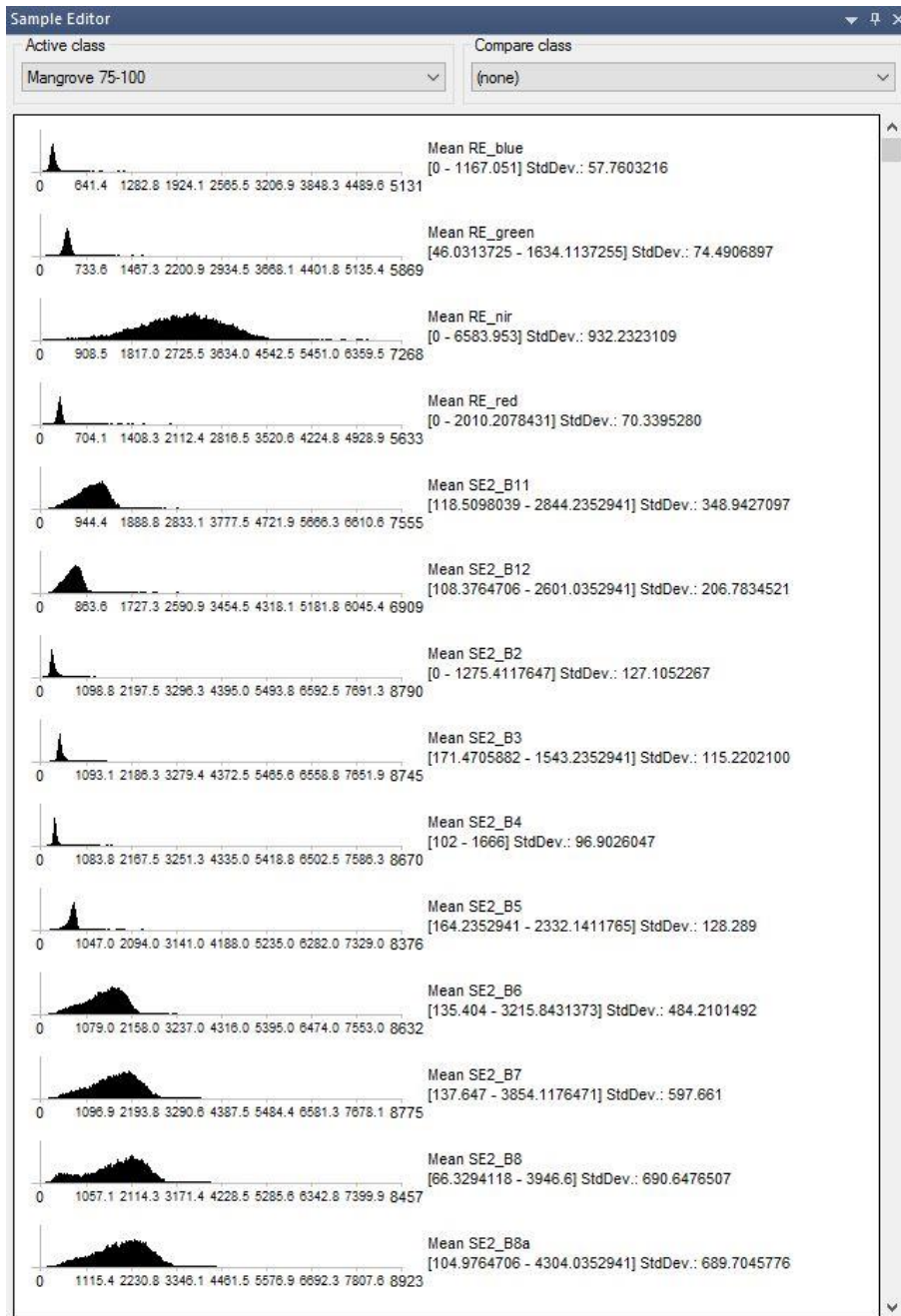
## Statistical parameters of the feature objects for the class Mangrove 50-75%



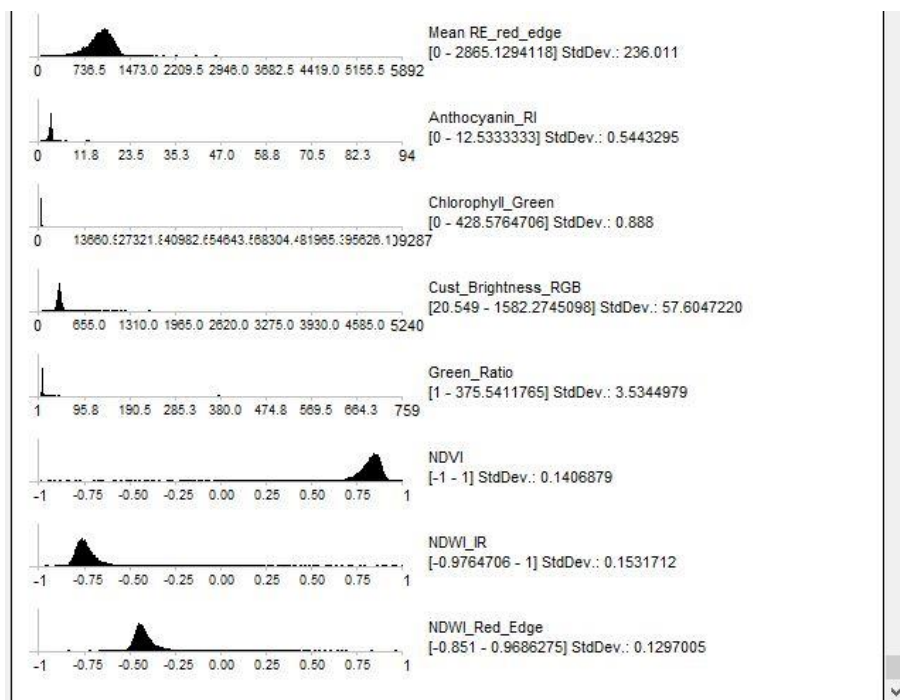
## Statistical parameters of the feature objects for the class Mangrove 50-75% cont.



## Statistical parameters of the feature objects for the class Mangrove 75-100%



## Statistical parameters of the feature objects for the class Mangrove 75-100% cont.

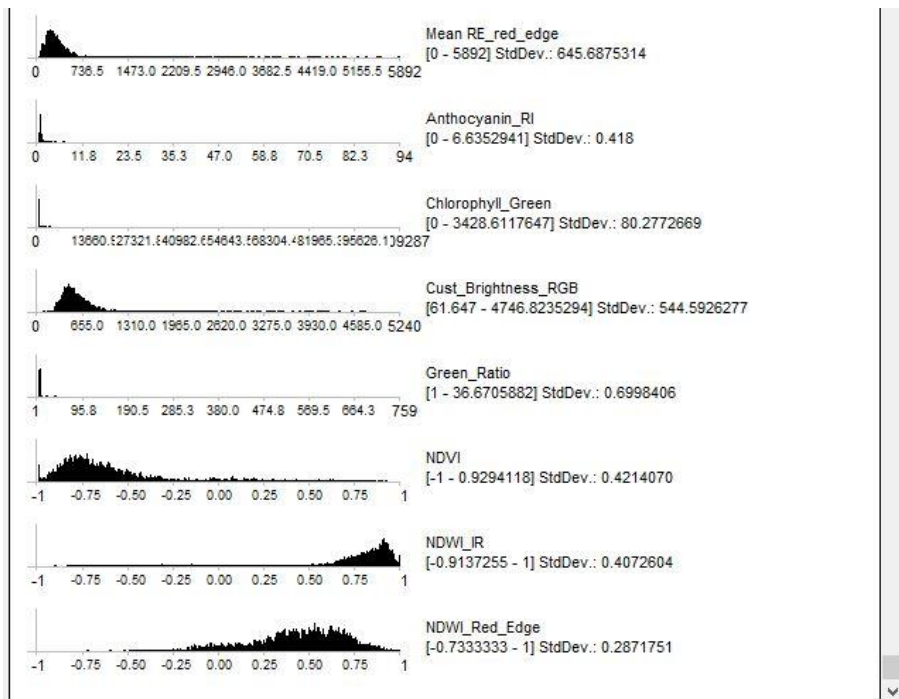


## Statistical parameters of the feature objects for the class Seagrass 0-50%

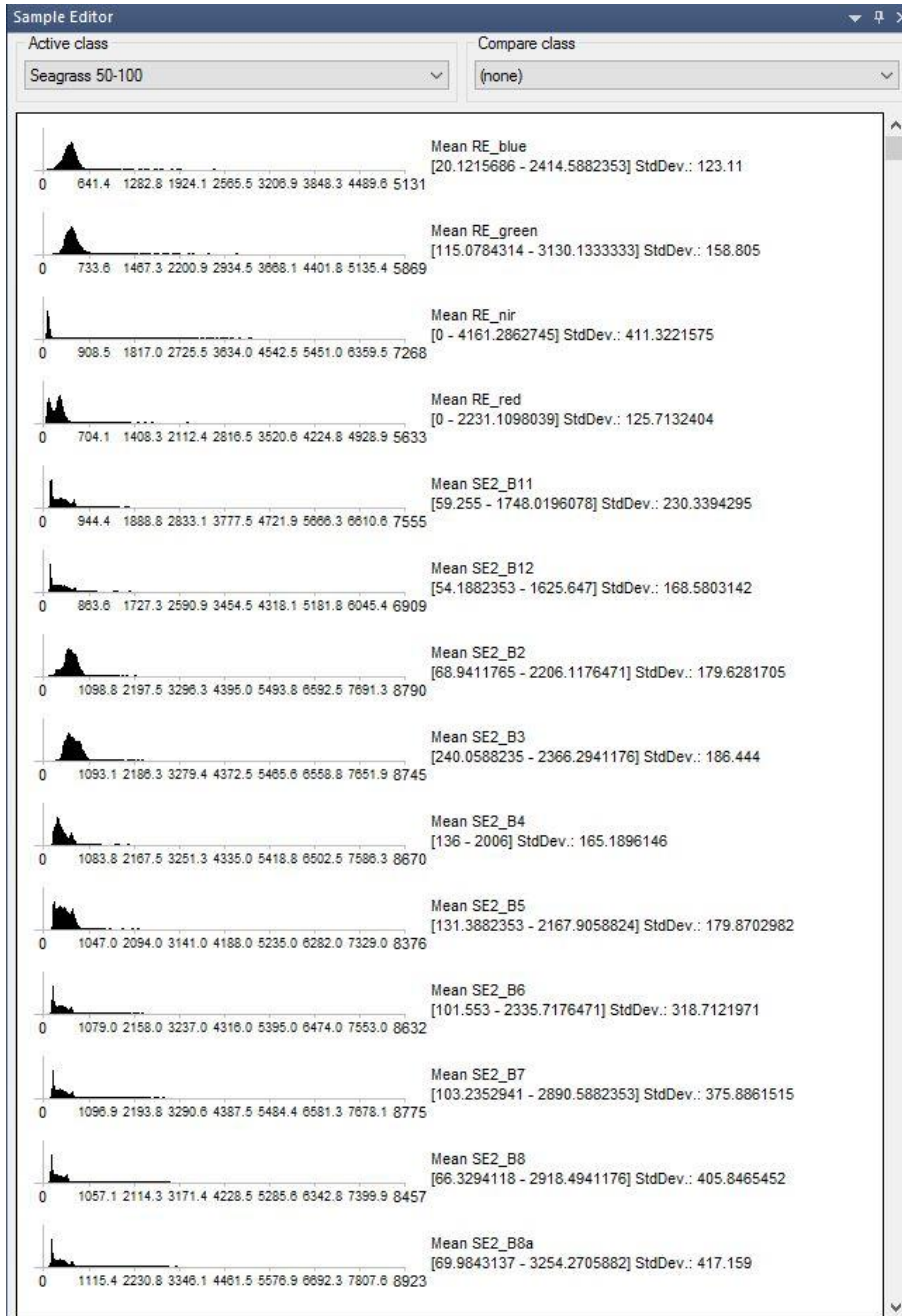




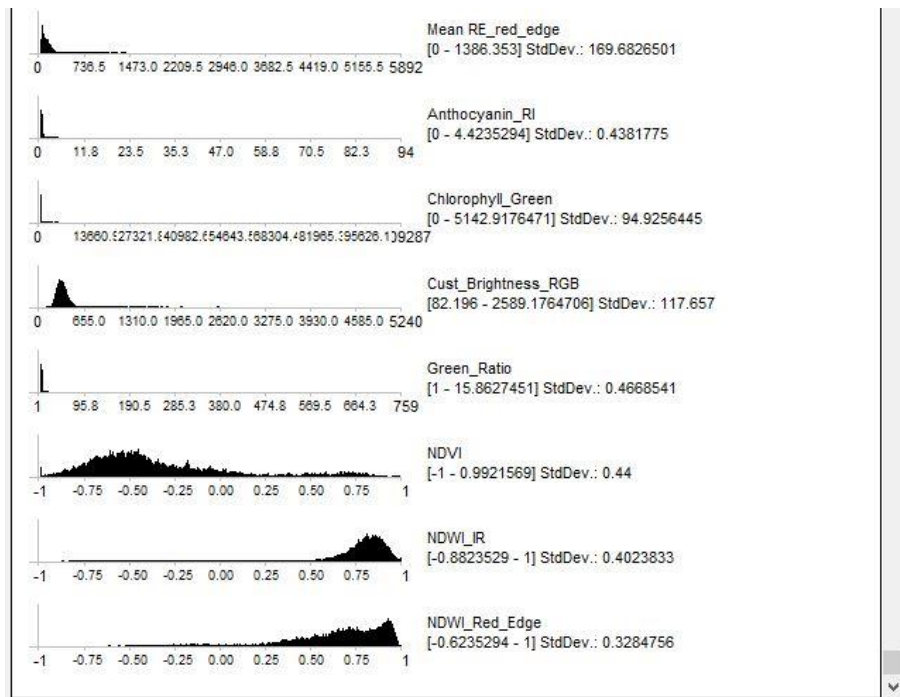
## Statistical parameters of the feature objects for the class Seagrass 0-50% cont.



## Statistical parameters of the feature objects for the class Seagrass 50-100%



## Statistical parameters of the feature objects for the class Seagrass 50-100% cont.



## Annex II

### Field sheet for terrestrial sample points

#### LCCS Field Sampling RSS GmbH; Mangroves

Site ID:				Date:	dd.mm.yyyy
				Time:	
Location:					
Surveyor:	GPS coordinates (UTM or lat/lon):	GPS point Nr.:	Photo Nr.:	North East South West Up	

Mangrove coverage (%)	Mangrove species	Mixed w/ sedge or grass <small>Just y/n</small>	Covered by other trees or palms <small>Just y/n</small>
-----------------------	------------------	--	--

**Please assess four mangrove coverage levels**

- 0% - 25%
- 25% - 50%
- 50% - 75%
- 75% - 100%

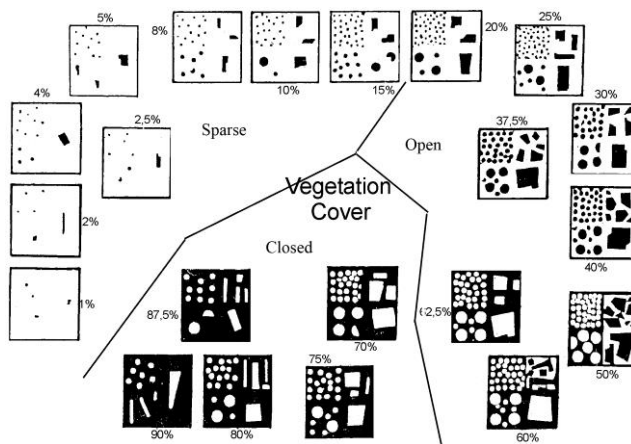
**Please take 5 photos per site, standing at the GPS point**

- One photo facing north, one facing east, south, west
- Fifth photo should be taken directly upwards (ie. pointed at the sky)

\*Locations with species taller than mangroves may be unuseable for accuracy assessment.

For a suggested location with more than 75% overgrowth coverage, consider relocating measurement point.

Comments: (anthropogenic impacts, transition zone, proximity to shore, etc.)
--



**Clarification:**

Everything which is dark is meant to represent canopy cover. When the background is black, as in the lower quadrats, the white objects then represent gaps in the canopy. Thus dark circles+rectangles can either represent individual trees or a stand of trees that have combined closed coverage, while the white objects represent areas where there is no canopy coverage.

## Field sheet for marine sample points

### LCCS Field Sampling RSS GmbH; Seagrass

Site ID:		Date:	dd.mm.yyyy
		Time:	
Location:			
Surveyor:	GPS coordinates (UTM or lat/lon):	GPS point Nr.:	Photo Nr.:

Depth (m)	Water clarity	Bottom type	Seagrass	Seagrass coverage (%)	Algae	Overall Coverage (%)
	Such as Secchi depth	e.g. rock, sand, pebble, etc.	Just y/n		Just y/n	

**Please assess four seagrass coverage levels**

0% - 25%

25% - 50%

50% - 75%

75% - 100%

\*Data on species level is not necessary, but you may assess it as well.

Comments: (anthropogenic impacts, near to river, plot characteristic for surroundings, etc.)
--

More information

<http://coralhealth.spatial.hawaii.edu/research.html>

[http://gulfsce.usgs.gov/gom\\_ims/sgpubs.html](http://gulfsce.usgs.gov/gom_ims/sgpubs.html)

<https://en.wikipedia.org/wiki/Seagrass>

### Seagrass Percentage Cover

